CHAPTER 2

Water Cycle

I. INTRODUCTION

The hydrologic cycle is an important feature of all ecosystems, and particularly forests, which generally grow in climates where precipitation provides more water than the vegetation can use or soils can store. The excess water contributes to stream flow, which provides for irrigation and urban needs far from the source of precipitation. Vegetation is a major factor in the hydrologic cycle, as shown in Fig. 2.1. Before precipitation reaches the soil, water is intercepted and evaporated from the surface of vegetation and the litter layer. The rate at which water infiltrates into the soil, runs off the surface, or percolates through to the water table is affected by the density and depth of root channels and organic residue incorporated into the soil.

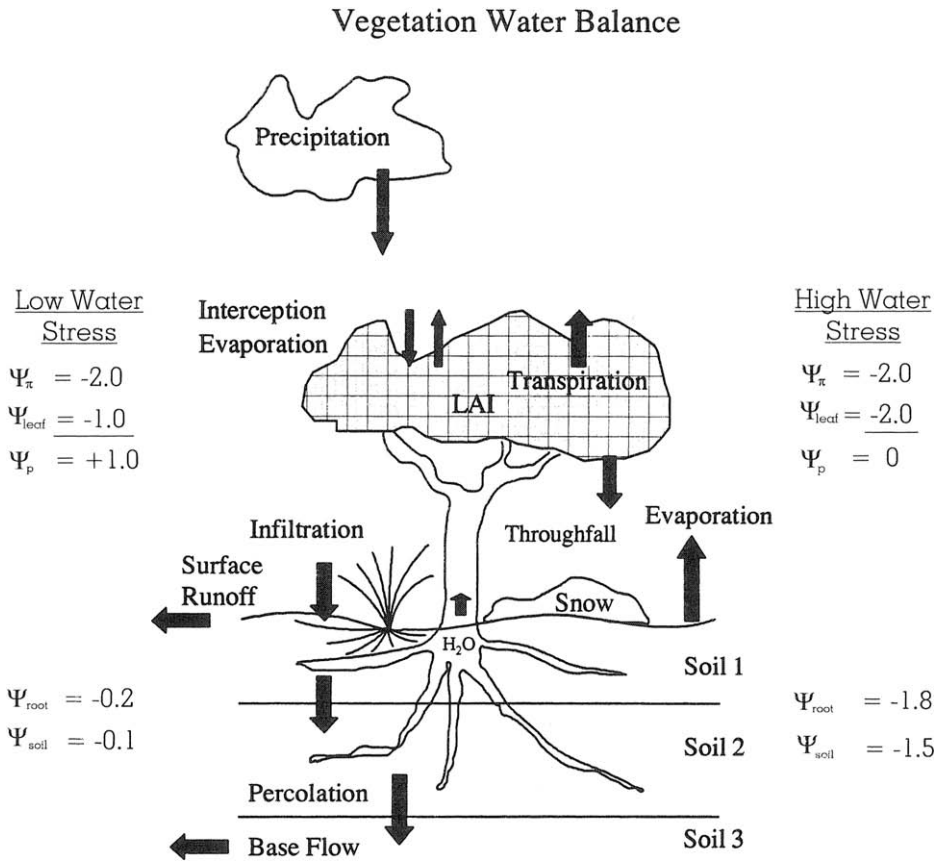

FIGURE 2.1. Stand water balance. Precipitation which falls as rain, snow, or fog is intercepted on vegetation; the amount intercepted depends to some extent on leaf area index (LAI). Some precipitation reaches the ground surface by throughfall and stemflow, wets the litter, runs off, or infiltrates into the soil where it may percolate to the water table. Some water is held against gravitational forces within the soil matrix; this is available for extraction by plant roots. Water taken up by plants may be stored temporarily within the stem, branches, and foliage, but most is transpired quite rapidly from the leaves into the atmosphere. Evaporation of water also occurs from plant and soil surfaces when they are wet. Example components of water potential for a tree under low and high stress are given. Note how leaves under high stress can have a pressure potential of 0.0 MPa causing wilting, and that the xylem pressure potential gradient from root to leaves is –0.8 MPa for the low stress example but only –0.2 MPa under high stress, quantifying reduced water flow rates that occur under high stress. See Section III,A for details of plant water potential. (After Neilson, 1995.)

Trees differ from other types of vegetation in their vertical height, which has important consequences for local climates because heat and water vapor transfer processes are strongly influenced by vegetation roughness, which is proportional to height. Trees also extend their roots deeper than many other types of vegetation and thus tap additional sources of water (Canadell *et al.*, 1996). The amount of water stored in the rooting zone often determines whether a stand of trees can continue to grow during a drought or whether mortality rates are likely to increase in association with outbreaks of disease and insects (Chapter 6).

Forest hydrologists are particularly interested in the fraction of precipitation that enters streams during storms, a component that may vary from <10 to >50% of annual streamflow and causes the majority of flooding, erosion, and transfer of pollutants to downstream areas (Johnson and Lindberg, 1992). By continuously measuring precipitation and streamflow in gauged watersheds, hydrologists have obtained empirical relations to answer many practical questions. Long-term studies at gauged watersheds, moreover, have provided baseline data for developing and testing a host of increasingly detailed process models that couple water, carbon, and nutrient cycles to changes in vegetation, climate, soils, and transfer of chemicals from the atmosphere (Bormann and Likens, 1979; Johnson and Lindberg, 1992). These process models, which will be featured in Chapter 8, have the advantage of more general applicability than empirical data but require more information than is commonly available.

In our search for general principles that apply across a range of scales, we emphasize the basic physics involved in water movement through the soil–plant–atmosphere continuum and indicate how specific measurements of climate, soils, and plant structural and physiological properties interact to affect the hydrologic cycle. A few basic equations are presented, supplemented with graphic presentations of important functional relationships. More formal mathematical treatments are provided in other texts (Monteith and Unsworth, 1990; Landsberg and Gower, 1997).

In this chapter we limit discussion to the hydrologic balance of forest stands over a period of 1 year. Using a simple energy balance approach, we first examine the rates of water loss by evaporation or transpiration from forests compared with other types of vegetation. We then consider the factors controlling interception and evaporation. Water vapor is lost from dry canopies by transpiration, which involves the limitations imposed by leaf stomata. A major section concerns the uptake of water from soil and its flow through stems and branches to leaves. From this analysis, we discover how the accuracy of ecosystem model predictions of seasonal water balances can be significantly improved by monitoring a few physiological properties of the vegetation, along with a select number of environmental variables. Consideration of water storage in soils and snow, together with surface runoff, infiltration, and percolation, completes the coverage of all basic processes. The major processes are coupled into a generalized hydrologic model that places structural limits on the kind of forests that can develop. These stand-level hydrologic models serve, with some modifications, as a basis for expanded analysis in time and space (Chapters 5, 8, and 9).

II. HEAT AND WATER VAPOR TRANSFER FROM VEGETATION

A. Energy Balance

The total flux of water vapor from an ecosystem can be estimated from the energy balance, determined by measuring the radiant energy absorbed and retained by the system (net radiation) and the mean gradients of temperature and humidity between the canopy upward to the atmosphere (Monteith and Unsworth, 1990). The radiation balance includes both short-wave (0.3–4 μm) and long-wave (4–80 μm) components of radiation. About 95% of solar radiation is short-wave, which contains about equal proportions of visible light (0.4–0.7 μm; the photosynthetically active component of radiation, PAR) and near-infrared

radiation (NIR). Short-wave radiation incident on vegetation or other surfaces may be reflected or absorbed; the absorbed radiation may heat the surface and be transformed into sensible heat, or it may evaporate water (latent heat). All surfaces above absolute zero emit long-wave radiation at a rate proportional to the fourth power of the temperature (Stefan–Boltzmann law). The total radiation incident on any surface is the sum of (1) direct short-wave radiation from the sun; (2) diffuse short-wave radiation from the sky; (3) reflected short-wave from nearby surfaces; (4) long-wave radiation from atmospheric emission; and (5) long-wave emitted from nearby surfaces (Fig. 2.2). Net radiation (R_n) is quantified according to the following equation:

$$R_n = (1 + \alpha)I_s - \varepsilon_L\, \sigma T^4 \text{ (surface)} + \sigma T^4 \text{ (sky)} \tag{2.1}$$

where α is the albedo or reflectivity of the surface as a fraction of intercepted incident short-wave radiation (I_s); ε_L is emissivity compared to a perfect black body, with ε_L for most soils and vegetation being between 0.9 and 0.98; σ is the Stefan–Boltzmann constant ($5.67 \times 10^{-8}\,\mathrm{W\,m^{-2}\,K^{-4}}$); and T is Kelvin temperature in reference to absolute zero (10°C = 283 K).

Depending on the reflective properties of leaves, the net radiation above dense forests is typically about 80–90% of incident short-wave radiation (Landsberg and Gower, 1997). If soils or snow intercept a major part of incoming solar radiation, more precise calculations are required, based on the fractions of short- and long-wave radiation that penetrate through the canopy. Reflectivities (*albedos*) for a wide range of surfaces are presented in Table 2.1.

The surface energy balance may be written

$$R_n + G = H + \lambda E \tag{2.2}$$

where R_n is the net radiant energy, in Joules (J) m^{-2} s^{-1} or Watts (W) m^{-2}; G represents soil and stem storage of heat (into the system during the day, out at night); H is the sensible heat flux into the atmosphere ($\mathrm{W\,m^{-2}}$); and λE represents the latent heat flux ($\mathrm{W\,m^{-2}}$), the energy used to evaporate water, where λ is the heat of vaporization of water ($2454\,\mathrm{kJ\,kg^{-1}}$ at 20°C) and E is the evaporation rate ($\mathrm{kg\,m^{-2}\,s^{-1}}$).

The available energy, represented by the difference in net radiation and soil heat flux, is dissipated almost entirely as either sensible or latent heat, with a small but important component going into metabolic activity (photosynthesis and respiration, Chapter 3). On a 24-hr basis, the storage term (G) is very small, but seasonally it is important because it may change in sign and cause soil to warm or to cool to considerable depth. The ratio of sensible to latent heat losses ($H/\lambda E$), termed the *Bowen ratio* (β), is an important ecosystem index in relation to how it varies diurnally and seasonally. If G in Eq. (2.2) is small, it may be neglected so that $R_n \approx \lambda E + H$. By definition, if $\beta = H/\lambda E$, then $\beta\lambda E = H$. By substituting for H in Eq. (2.2), $R_n = \beta\lambda E + \lambda E = \lambda E(1 + \beta)$, and hence we can predict latent heat loss with the Bowen ratio and net radiation:

$$\lambda E = R_n/(1 + \beta). \tag{2.3}$$

Short vegetation, such as a well-watered pasture, maintains a fairly constant Bowen ratio throughout the day, with both latent and sensible heat transfer essentially tracking net radiation. The Bowen ratio above a well-watered forest, on the other hand, exhibits

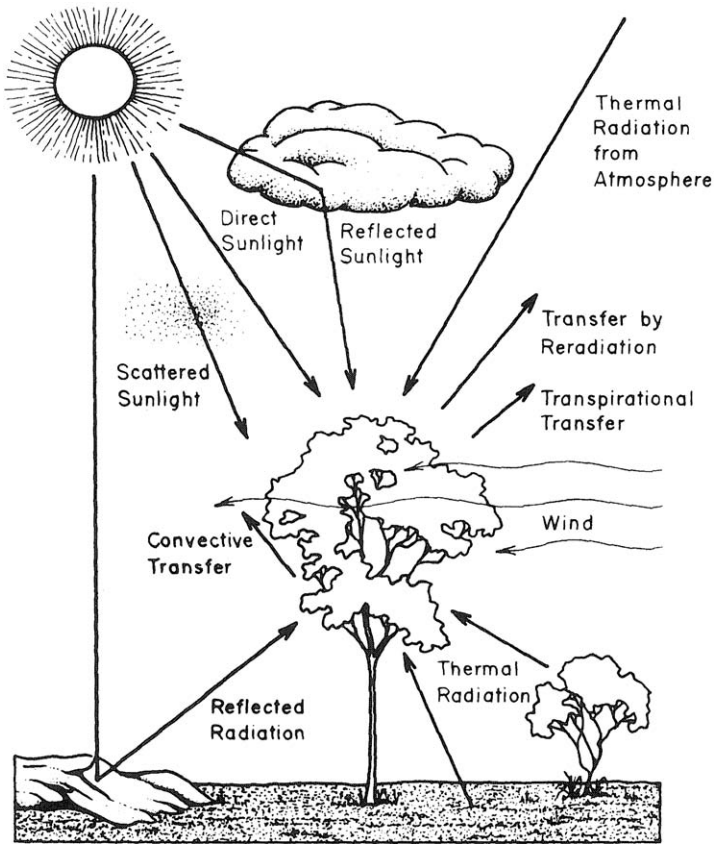

FIGURE 2.2. Energy exchange between vegetation and the environment involves a number of processes. Solar radiation reaches plant canopies as direct, scattered, and reflected sunlight, all of which contain some short-wave components important for photosynthesis. On partly cloudy days, reflection from clouds can increase incident short-wave radiation at the ground surface by as much as 30%. On clear days, less than 10% of the short-wave radiation is scattered by the atmosphere; on overcast days, incident short-wave radiation is reduced and diffuse, casting no shadows. Plant and other surfaces absorb and reflect short-wave and long-wave radiation, and they emit thermal radiation as a function of their absolute (Kelvin) temperature. The bulk of the heat load on plants is reradiated; evaporative cooling by transpiration and heat transfer by convection and wind (advection) remove the rest. Some heat is stored temporarily in the soil and plant tissue, which is later reradiated. (After Gates, 1980.)

considerable diurnal variation. For example, in Fig. 2.3, in the early morning (0600 hr), $\beta \leq 0.01$ associated with the rapid evaporation of dew; at 1000, with dry surfaces, β is near 1.0, which indicates that sensible and latent heat transfer are equal at about 250 $W\,m^{-2}$, with the latter equivalent to about 0.36 $mm\,hr^{-1}$, whereas by 1400, after the peak solar radiation, β increases to nearly 1.9 as a result of physiological limitations on transpiration (Price and Black, 1990). For more insight into interpretation of the diurnal variation in H and λE, we need information on whether the canopy is wet or dry and other properties that affect exchange rates.

TABLE 2.1
Reflectivity (Albedo) of Various Surfaces[a]

Surface	Albedo
Forests	0.05–0.18
Grass	0.22–0.28
Crops	0.15–0.26
Snow (old–new)	0.75–0.95
Wet soil	0.09 ± 0.04
Dry soil	0.19 ± 0.06
Water	0.05 to >0.20

[a]After Jones (1992) and Lowry (1969).

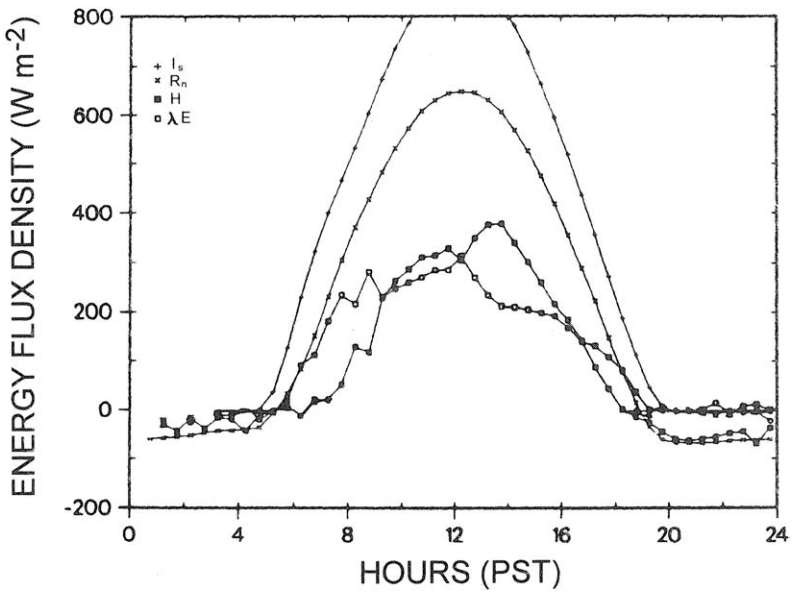

FIGURE 2.3. Ecosystem energy exchange balance for a Douglas-fir stand in British Columbia for a clear day in July. Variation in incoming short-wave radiation (I_s), net radiation (R_n), heat storage (G), and fluxes of sensible heat (H) and latent heat (λE) are presented for a 24-hr period. The Bowen ratio ($H/\lambda E$) was small in early morning as dew evaporated freely from leaf surfaces. From 0800 to 1200 transpiration dissipated nearly as much energy as was lost through sensible heat transfer (Bowen ratio approximately 1.0). During midafternoon, partial closure of leaf stomata reduced λE and increased the Bowen ratio to nearly 2.0. (Modified from *Agricultural and Forest Meteorology,* Volume 50, D. T. Price and T. A. Black, "Effects of short-term variation in weather on diurnal canopy CO_2 flux and evaporation of a juvenile Douglas-fir stand," pp. 139–158, 1990, with kind permission of Elsevier Science–NL, Sara Burgerhartstraat 25, 1055 KV Amsterdam, The Netherlands.)

B. Evaporation from Wet Surfaces

In this section we provide background on the historical development of equations describing evaporation, borrowing from portions of an excellent review paper written by Kelliher and Scotter (1992). Evaporation involves the diffusion of water vapor molecules away from wet surfaces and is proportional to the difference between the saturated vapor pressure of water (determined by water temperature) and the vapor pressure of the air (a function of air temperature and humidity). The amount of water vapor held in a saturated atmosphere increases exponentially with temperature (Fig. 2.4); the degree of saturation is often expressed as the *relative humidity.* The *dew point* is the temperature at which the water vapor pressure equals the saturated vapor pressure; below that temperature, condensation occurs. Where water vapor pressure cannot be measured directly, it is often approximated from a correlation with minimum night temperatures (Chapter 7). The *water vapor pressure deficit* (*D*) is an important term in many models of evaporation and represents the difference between the vapor pressure at saturation and the actual vapor pressure, determined by the amount of water vapor in the air (Jones, 1992).

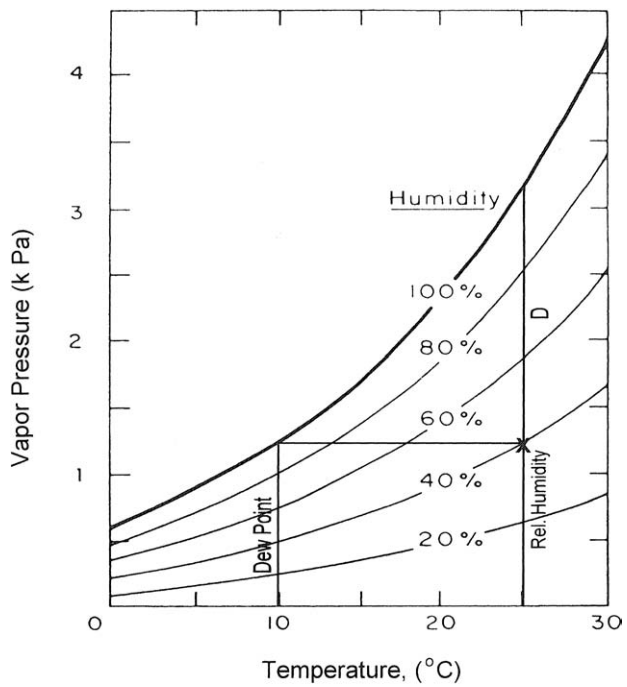

FIGURE 2.4. The amount of water vapor that may be held in the air increases exponentially with temperature. The saturated vapor pressure (e_{sat}) between 0° and 45°C when expressed in kilopascals (kPa) is approximated as a function of air temperature (T) as $e_{sat} = 0.61078 \exp[(17.269T)/(237 + T)]$. The water vapor deficit of the air (D) is the difference between the saturated value and that actually held at a given temperature. In this example, air at 25°C with a relative humidity of 40% must be cooled to 10°C to reach the dew point. The vapor pressure deficit (D) is the difference between e_{sat} at 25°C (3.2 kPa) and that at the dew point (1.2 kPa), or 2.0 kPa.

Only if the air is absolutely still does molecular diffusion alone control the rates of evaporation. Most of the time, the air circulates over forests and other natural surfaces causing turbulence that greatly enhances the potential for evaporation. Immediately adjacent to a solid surface the air is still, but away from that surface wind movement causes drag, just as moving water does on objects in a stream. As the momentum increases, eddies and currents are formed. Turbulence is increased if the underlying surface is rough, as is the case for forests compared to the surface of a lawn. Dalton in 1801 first recognized the importance of including turbulence in estimating evaporation (cited in Kelliher and Scotter, 1992). Turbulence is expressed in an aerodynamic transfer equation, generally expressed as

$$E = (e_w - e_a)\, f(u) \tag{2.4}$$

where E is evaporation rate, e_w is saturated vapor pressure of water at the surface temperature, e_a is vapor pressure of the air, and f is an empirical function that describes the aerodynamic exchange property of the surface as a function of air circulation (turbulence) associated with wind speed (u).

Evaporation, as we have shown in presenting the Bowen ratio, is a component of the energy balance. In 1948, Penman combined the energy balance with Dalton's equation to calculate evaporation rates without needing to know the surface temperature. In its modern form the Penman equation can be written (Monteith and Unsworth, 1990)

$$E = E_{eq} + Dg_b/\zeta. \tag{2.5}$$

In Eq. (2.5), E_{eq} is the evaporation rate ($m\,s^{-1}$) obtained in equilibrium with an extensive, homogeneous wet surface via the energy balance (McNaughton, 1976) and is given by

$$E_{eq} = \frac{\varepsilon}{\rho\lambda(\varepsilon+1)} R_n \tag{2.6}$$

where ρ is the density of air and λ is the latent heat of vaporization, defined earlier, both properties of water in air and only weakly temperature dependent; ε is the change of latent heat relative to the change of sensible heat of saturated air which is 1.26 at 10°C and increases exponentially with temperature (T): $\varepsilon = 0.7185\, e^{0.0544T}$. Other terms in Eq. (2.5) are the air saturation deficit D (Pa) and g_b, the boundary-layer conductance for water vapor ($m\,s^{-1}$), which approaches zero under calm conditions, increases with wind speed, and depends on the roughness of the evaporating surface (Fig. 2.5). Zeta (ζ), the final term in Eq. (2.5), is a combination function so that $\zeta = \rho(\varepsilon + 1)G_vT_k$, where G_v is the gas constant for water vapor ($0.462\,m^3\,kPa\,kg^{-1}\,K^{-1}$) and T_k is air temperature in degrees Kelvin.

The relative importance of E_{eq} and Dg_b/ζ in Eq. (2.5) depends on the relative magnitudes of net radiation and boundary-layer conductance. When the boundary-layer conductance is small, the deep boundary layer largely isolates the wet surface from the effects of the saturation deficit in the air above, and evaporation rates approach the equilibrium rate E_{eq}. Alternatively, the energy for evaporation may be increased substantially if *advection* provides for the horizontal transfer of warmer and drier air into the system by increasing the saturation deficit D (Fig. 2.4).

The rate of evaporation from wet surfaces depends strongly on the boundary-layer conductance (g_b). Representative values of boundary-layer conductance for pasture, crops, and forests, with closed canopies and nominal heights of 0.05, 0.5, and 20 m, respectively,

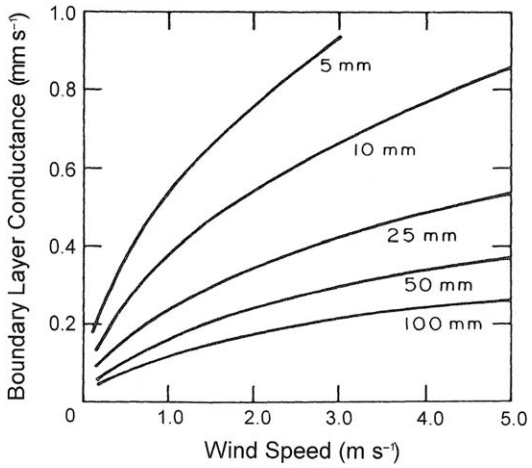

FIGURE 2.5. The aerodynamic or boundary-layer conductance (g_b) is generally high for tall vegetation because of turbulence. With shorter vegetation, however, less turbulence is present, and the width of leaves (shown from 5 to 100 mm) and wind speed become increasingly important in determining g_b. (After Grace, 1981.)

are 0.01, 0.02, and 0.2 m s^{-1}. Differences in what approaches maximum wet canopy evaporation rates for the three types of vegetation can be illustrated using typical daytime values during periods of rainfall, for the variables in Eq. (2.5): 50 W m^{-2} for R_n, 0.1 kPa for D, 10°C for air temperature, and the g_b values given above. These give evaporation rates of 0.05 mm hr^{-1} for the pasture, 0.065 mm hr^{-1} for crops, and 0.3 mm hr^{-1} for the forest. At night, evaporation continues at nearly the same rate for forests (assuming D remains at 0.1 kPa), adding up to a maximum 24-hr water loss of nearly 6 mm day^{-1}. Shorter vegetation is more dependent on the net radiation balance, which is negative at night, so maximum daily rates are unlikely to exceed 1–1.5 mm day^{-1}, unless the vegetation is situated on exposed sites where wind speeds are sufficient to increase the boundary-layer conductance to values similar to that typical for forests (Fig. 2.5).

Evaporation from bare soil, which has a boundary-layer conductance similar to a pasture, may also reach 6 mm day^{-1} on sunny summer days, hut these rates are soon reduced as the surface dries (Kelliher and Scotter, 1992). The litter layer beneath a dense forest, which may store two to three times its dry mass in water (10,000 kg of water per hectare is equivalent to 1 mm), is shielded from direct radiation and wind turbulence so normally contributes less than 5% to daily evaporation (Waring and Schlesinger, 1985). When the canopy is more open, however, turbulent exchange and direct radiation on the understory vegetation and leaf litter increase substantially and losses from these surfaces can account for up to 30% of the daily total. As these surfaces dry, solar radiation begins to heat the air, which results in increasing the air saturation deficit.

C. Interception

In the previous section we established that maximum rates of evaporation from the wet surface of various (homogeneous) types of vegetation and from bare soil could, under

specified conditions, reach 6 mm day^{-1}. Actual rates of evaporation, however, are generally much less. One way of assessing the evaporative losses from forest canopies is to determine the fraction of annual precipitation that falls but does not reach the ground. This fraction, termed *interception,* ranges from 10 to 50% of annual precipitation (Kelliher and Scotter, 1992).

The proportion of rainfall intercepted has been determined for a variety of forests by placing measuring devices in the open and at random points beneath the canopy. Other collectors placed around the stems of trees estimate stemflow. A summary of equations for computing throughfall and stemflow from measurements of gross rainfall is presented in Table 2.2. These calculate average values when the canopy is fully developed. Variation in interception can also be expected depending on the intensity and duration of a storm.

The storage capacity of a canopy can be estimated from interception calculated from equations presented in Table 2.2. For a plantation of Scots pine, Rutter (1963) found that the leafy shoots retained an amount of water approximately equal to the dry weight of foliage. Storage of precipitation on foliage, branches, and stems was estimated to be 0.8, 0.3, and 0.25 mm, respectively. Deciduous trees in general store less water on their canopies than conifers, unless the canopy is heavily loaded with epiphytes. If the precipitation is in the form of snow or ice, the water equivalent stored may be more than double that in the liquid state (Zinke, 1967).

Large deviations from these values occur in different seasons. The distribution of storage also changes with stand development because the surface areas of branches (living and dead) and stems increase with stand age up to a point, then decrease (Chapter 5). Epiphytes (mosses, lichens, liverworts) on branches and stems can greatly increase the capacity of those structures to absorb surface water, which explains, in part, why some large trees may exhibit almost no stemflow even during intense storms. Another factor that controls stemflow is the smoothness of the bark surface. Species with smooth surfaces such as beech (*Fagus*) may transport as much as 12% of the precipitation as stemflow, whereas pine normally transfers less than 2% by this route. Stemflow may have special

TABLE 2.2
Summary of Equations for Computing Throughfall and Stemflow for Coniferous and Hardwood Forests from Measurement of Rainfall[a]

Vegetation	Throughfall	Stemflow	Interception per 1 cm of rain
Red pine	$0.87P - 0.04$	$0.02P$	0.15
Loblolly pine	$0.80P - 0.01$	$0.08P - 0.02$	0.15
Shortleaf pine	$0.88P - 0.05$	$0.03P$	0.14
Ponderosa pine	$0.89P - 0.05$	$0.04P - 0.01$	0.13
Eastern white pine	$0.85P - 0.04$	$0.06P - 0.01$	0.14
Pine (average)	$0.86P - 0.04$	$0.05P - 0.01$	0.14
Spruce–fir–hemlock	$0.77P - 0.05$	$0.02P$	0.26
Hardwoods, in leaf	$0.90P - 0.03$	$0.041P - 0.005$	0.10
Hardwood, deciduous	$0.91P - 0.015$	$0.062P - 0.005$	0.05

[a]After Helvey (1971) and Helvey and Patric (1965). Last column presents estimates of interception for 1 cm of precipitation, where Interception = 1 − (Throughfall + Stemflow).

significance in distributing potassium to the area around certain smooth-barked trees, because that nutrient is easily leached from foliage (Gersper and Holowaychuk, 1971; Chapter 4). It may also concentrate water near the roots of some arid forest species, such as *Acacia aneura* (Doley, 1981). Details of this type are significant in explaining the composition of forests, but they cannot be incorporated into generalized models predicting interception.

Most hydrologic models that directly consider exchange of water vapor from vegetation incorporate some estimate of canopy leaf area. Detailed studies show that the capacity of foliage to store water increases in direct proportion to the surface area, although the retention coefficient (kg water per m^2 of surface) varies with leaf dimensions, orientation, and surface smoothness (Fig. 2.6). A reasonable estimate of the surface area of foliage, branches, and stems may be calculated from regressions with stem diameter (Chapter 3); however, because the amount of foliage present may vary by 100% throughout the year, indirect ways of estimating seasonal variation in the canopy surface area, expressed as the

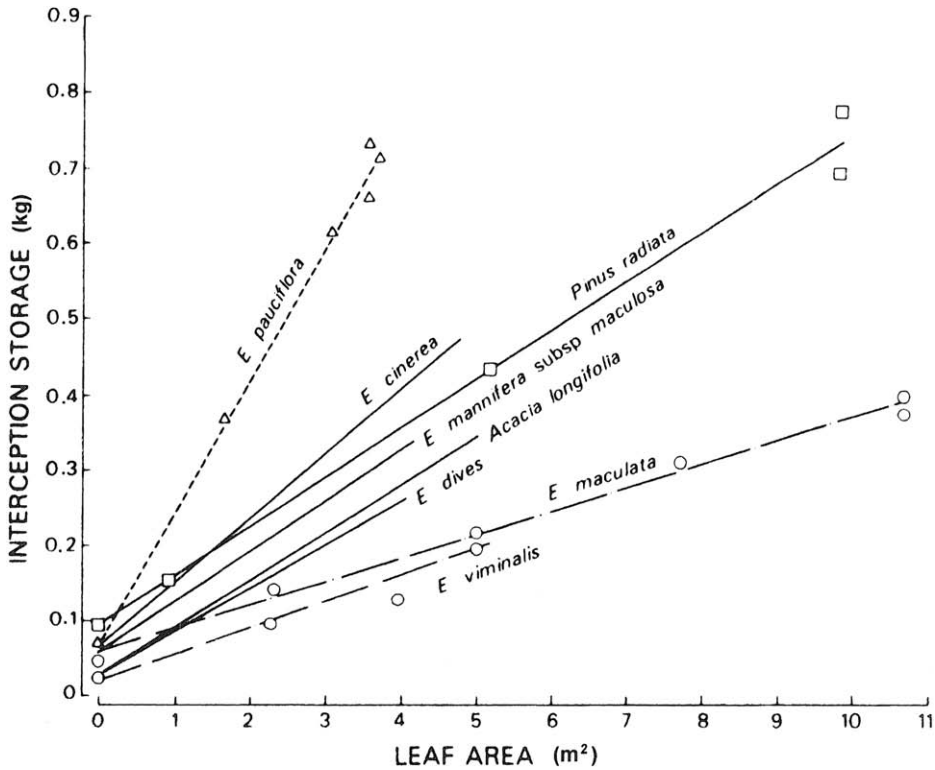

FIGURE 2.6. Interception storage capacity of six species of eucalyptus varying from 0.032 to 0.178 mm per unit leaf area, depending on surface properties and leaf orientation. *Acacia longifolia* and *Pinus radiata* had intermediate interception capacities. (Modified from *Journal of Hydrology,* Volume 42, A. R. Aston, "Rainfall interception by eight small trees," pp. 383–396, 1979, with kind permission of Elsevier Science–NL, Sara Burgerhartstraat 25, 1055 KV Amsterdam, The Netherlands.)

projected (or silhouette) area of leaves per area of ground surface [leaf area index (LAI)], have been sought.

D. Seasonal Estimation of Leaf Area Index

Leaf area index is defined as the projected area of leaves over a unit of land ($m^2\,m^{-2}$), so one unit of LAI is equivalent to $10{,}000\,m^2$ of leaf area per hectare. Sometimes LAI is expressed on the basis of all leaf surfaces. For broadleaf trees, the total is twice the projected area; for needle-leaf trees the conversion is between 2.4 and 2.6 (Waring *et al.,* 1982) and only rarely pi (π), because leaves are seldom perfect cylinders (Grace, 1987).

Seasonal variation in LAI may be estimated by determining a mid-season maximum value and then reducing this in proportion to the amount of leaf litterfall collected periodically throughout the year (Burton *et al.,* 1991). The most common method of estimating seasonal variation in LAI is from measurements of the fraction of visible light transmitted through the canopy to the ground (Pierce and Running, 1988; Gower and Norman, 1991). The *Beer–Lambert law* is often applied to calculate the fraction of light intercepted (I) by increasing layers of leaves:

$$I = 1 - Q_t/Q_o = 1 - e^{(-k)(\mathrm{LAI})} \tag{2.7}$$

where Q_o is the visible radiation on cloudless days incident above the canopy, Q_t is visible radiation transmitted through accumulated layers of leaves, and k is an extinction coefficient (usually between 0.3 and 0.6), which represents the fraction of visible radiation intercepted by a unit area of leaves. The relation is exponential, so that at $k = 0.5$, a LAI of 1, 3, 6, and 9 intercepts, respectively, 39, 78, 95, and 99% of the visible light. The Beer–Lambert law can also be applied to estimate the interception of near-infrared radiation by canopies. Because leaves are relatively transparent to infrared radiation, the shortwave radiation deep in plant canopies is relatively enriched in the near-infrared component, with k values often half those recorded for visible light (Jones, 1992).

In more open canopies, the vertical and horizontal distribution of leaves becomes important because certain configurations alter the normal exponential decrease in the net radiation and wind speed from the top of a canopy downward (Shuttleworth, 1989). *Roughness length* is a term related to boundary-layer conductance that describes how height and other structural features of vegetation modify the generally logarithmic wind profile through canopies and defines the height above the ground surface where wind speeds extrapolate to zero (Monteith and Unsworth, 1990). Roughness length and related expressions of how vegetation affects momentum transfer are important in estimating wet and dry fall of chemicals (Chapter 4) and in describing turbulence created by variations in vegetation and topographic conditions across landscapes (Chapter 8).

E. Modeling Evaporation

Evaporation occurs only from the wet surfaces of foliage, branches, stems, and litter or, when litter is absent, from the surface soil. Detailed models account for the storage and movement of water through ecosystems, estimating evaporation as a function of location of the wetted surfaces, energy loading, and other factors that affect the rate at which water

vapor is transferred to the atmosphere (Rutter *et al.,* 1971). Foliage temperature is lower when evaporation occurs and approaches air temperature when completely dry, a fact which permits the fraction of wet/dry foliage in a canopy to be estimated from direct or indirect measurements of the difference between temperatures of the canopy surface and air (Teklehaimanot and Jarvis, 1991).

To apply the Penman equation to partially wet canopies, Rutter (1975) developed a model that keeps continuous account during a storm of the fraction of surfaces that are wet and estimates evaporation exclusively from those surfaces. The position of the wet surfaces is important, as mentioned previously, because both the net radiation and wind speed are generally reduced exponentially from the top of the vegetation downward through layers of leaves (Shuttleworth, 1989). When gaps appear in a forest canopy, large eddies are created that increase turbulent transfer between the top of the canopy and the soil. Turbulent transfer around individual trees increases linearly as the spaces between trees become greater, but the boundary-layer conductance of the whole canopy approaches an asymptote as leaf area index increases (Teklehaimanot and Jarvis, 1991).

Gash (1979) modified Rutter's model so that it could be applied to estimate interception during storms of known average intensities ($\mathrm{mm\,hr^{-1}}$) by accounting for evaporation, throughfall, and stemflow. This kind of model can be applied to situations where only daily estimates of precipitation are available, but average rainfall intensities must still be known because 6 mm of light drizzle may be fully evaporated whereas a cloudburst of similar magnitude may result in only 1–2 mm being intercepted.

F. Transpiration from Plant Canopies

When the surfaces of leaves are dry, water loss takes place by transpiration through stomata. Plants can control stomatal opening and thus influence transpiration rates. By including a stomatal conductance term, Dalton's equation can be extended to calculate transpiration from a single leaf, and in 1965 Monteith used this approach to extend Penman's equation so that it could describe transpiration from a plant canopy using a single bulk canopy conductance (G_s) that is the product of the mean stomatal conductance (g_s) and LAI. The so-named Penman–Monteith equation may be written (McNaughton and Jarvis, 1983) as

$$E_T = \Omega E_{eq} + (1 - \Omega)E_{imp} \tag{2.8}$$

where transpiration (E_T) from a dry canopy is related to the evaporation rate (E_{imp}) imposed by the effects of the air saturation deficit D:

$$E_{imp} = Dg_s / \rho G_v T_k \tag{2.9}$$

and the coefficient Ω indicating the degree of coupling between the canopy and D is

$$\Omega = \frac{1+\varepsilon}{1+\varepsilon+g_b/G_S}. \tag{2.10}$$

The Penman–Monteith equation incorporates and defines the relative importance of the two environmental driving forces on evaporation, namely, net radiation (R_n), and the dryness of the air (D), with two controls: one physical, the boundary-layer conductance

(g_b), and the other physiological, the canopy stomatal conductance (G_s). When the boundary-layer conductance is much less than canopy conductance, Ω approaches 1, and transpiration rates approximate the equilibrium evaporation rate. This tends to be true for short vegetation; however, for tall vegetation, such as forests, the boundary-layer conductance usually exceeds canopy conductance, so that Ω approaches zero. Under such conditions, where other factors do not limit stomatal conductance, the air saturation deficit (D) rather than net radiation largely controls the rate of transpiration.

At LAI < 3, evaporation from the soil surface contributes greatly to the bulk conductance, but at LAI > 3, the canopy stomatal conductance (G_s) plays the dominant role. Körner (1994) published a distillation of leaf stomatal conductance (g_s) values for over 20 vegetation types and 200 species that showed maximum values were similar for most woody plant communities, at about $0.006\,m\,s^{-1}$. Kelliher *et al.* (1995) expanded the comparison to include maximum whole canopy conductance (G_s) and concluded that forests with LAI > 3.0 have nearly stable maximum G_s values (about three times the maximum g_s, see Table 9.3), because the maximum g_s of individual leaves progressively decreases with additional increments of LAI (Lloyd *et al.,* 1995; Whitehead *et al.,* 1996).

G. Empirical Model of Stomatal Conductance

The Penman–Monteith equation requires estimates of stomatal conductance in order to predict transpiration from canopies. Stomatal conductance is often predicted as a function of environmental factors which directly or indirectly restrict stomata opening below a maximum (g_{max}), so that

$$g_s = g_{max}\, f_1(L)\, f_2(T)\, f_3(D)\, f_4(H_2O)\, f_5(CO_2). \tag{2.11}$$

The variables $f_1, f_2, \ldots, f_x$ vary from 0 to 1 and are nonlinear functions of light (L), temperature (T), water vapor pressure deficit (D), available soil water (H_2O), ambient CO_2 concentrations, and air pollutants (Chapter 6). Equation (2.11) describes a response surface that may be defined by leaf–gas exchange measurements under controlled conditions or by determining the maximum G_s observed for whole canopies over a wide range of conditions (Jarvis, 1976). Lloyd *et al.* (1995) constructed a series of response surfaces showing interactions between light, leaf temperature, and air vapor pressure deficits on G_s from continuous monitoring of water vapor exchange above a tropical forest (Fig. 2.7a). With these empirical relations, measured canopy stomatal conductance was accurately predicted (Fig. 2.7b). The canopy stomatal responses shown in Fig. 2.7a are similar to those obtained for other types of forests, although the air temperature response is much less pronounced for temperate and boreal forests (Shuttleworth, 1989).

The most striking feature of the canopy stomatal response patterns illustrated in Fig. 2.7 is the limitation that the foliage to air vapor pressure gradient exerts as radiation and temperature increase. Between values for D of 0.5 to 3.0 kPa, canopy stomatal conductance is reduced exponentially. It is primarily because of this reduction in G_s associated with increasing D that transpiration rates from forests, even on clear days, rarely exceed $0.5\,mm\,hr^{-1}$ or $6\,mm\,day^{-1}$ (Kelliher *et al.,* 1995). If stomata were not to close in response to D, transpiration could theoretically be expected to exceed $30\,mm\,day^{-1}$ in some situations.

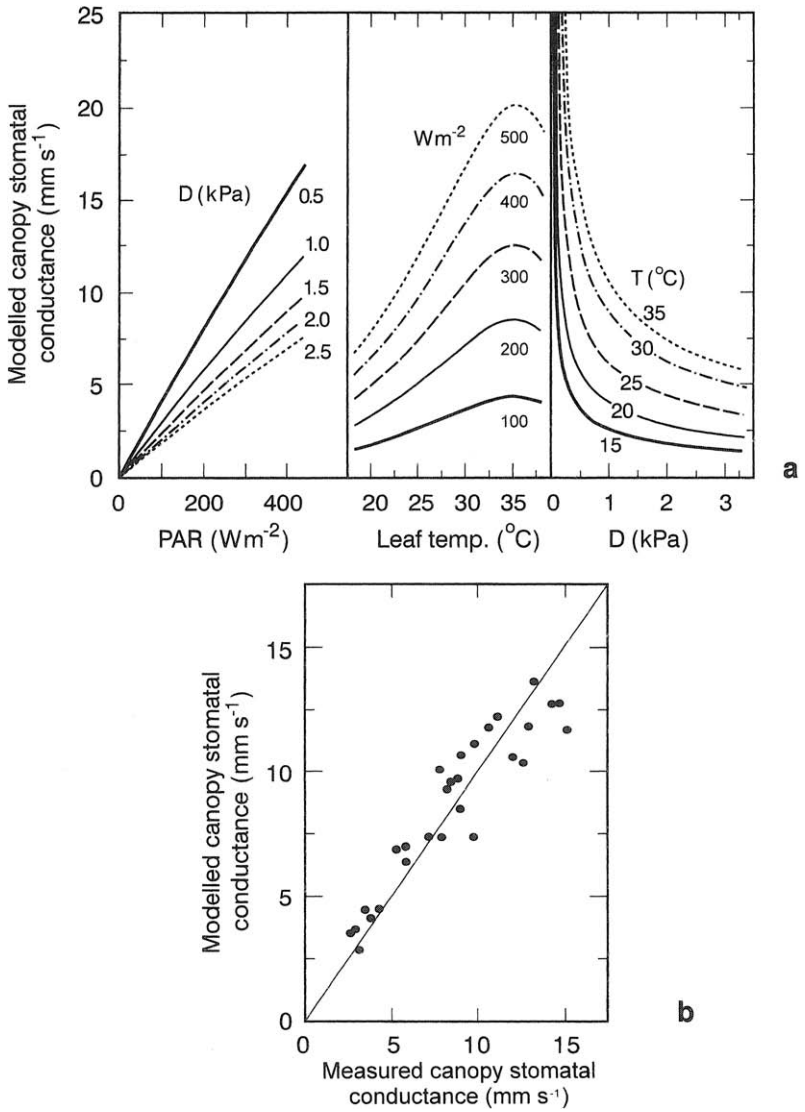

FIGURE 2.7. (a) Empirical data collected above an Amazonian rain forest illustrate that canopy stomatal conductance (G_s) varies with meteorological conditions. in general, G_s increases with photosynthetically active radiation (PAR) and air temperature (T) and decreases with vapor pressure gradient between foliage and the air (D). (b) Combined into a model, predicted canopy stomatal conductance closely matched that measured. (After Lloyd *et al.,* 1995.)

The empirical approach to modeling stomatal response has been widely applied in comparative studies to document differences among species in their sensitivity to various environmental factors. This type of information is useful in predicting changes in forest composition if supplemented with additional information regarding differential growth allocations and sensitivity to various types of disturbances (Chapters *5* and 6). Although

empirical models provide good predictions locally, they should not be extrapolated to situations where environmental conditions are outside those studied. In Chapter 3, where the process of photosynthesis is discussed, more basic models of stomatal response will be introduced that incorporate biochemical constraints (von Caemmerer and Farquhar, 1981; Leuning *et al.,* 1995).

The preceding sections have provided an outline of the energy balance principles that govern evaporation from vegetation and the ground surface. The Penman–Monteith or combination equation allows calculation of transpiration from dry canopies; Eqs. (2.8) and (2.10) can be used to show how forests differ from other vegetation types. The Penman–Monteith equation is generally employed in most present-day ecosystem models to predict transpiration and also evaporation, the latter by setting G_s to infinity.

III. WATER FLOW THROUGH TREES

A. Plant Hydraulic Limitations on the Flow of Water through Trees

Hydraulic restrictions on the rate at which water flows through stem wood, branches, and stomata place direct limits on transpiration (see Meinzer and Grantz, 1991; Mott and Parkhurst, 1991) and affect how tall trees may grow, even in environments well supplied with water. Some species are better adapted than others in maintaining the integrity of the water conducting pathway between roots and leaves. In this section, we briefly describe how water flows upward through the vascular system, where the major resistances to flow occur, and the consequences of changes in the internal water status of trees on stomatal conductance and leaf area.

Liquid water moves from the soil through roots upward in vascular tissue (*xylem*) in which nonliving cells with heavily thickened, lignified walls serve as conduits. The conducting cells in the xylem are stable in their dimensions; only if the relative water content drops below about 20% does shrinkage occur and cause wood to split (Siau, 1971). Anatomically, the water conducting elements differ between gymnosperms and angiosperms. Gymnosperms have short *tracheids* that interlock and exchange water through bordered pits with functional valves on side walls. Angiosperms have longer and wider and more efficient conducting elements (*vessels*), which are interconnected at their ends by perforated plates. Under conditions where water columns break, tracheids are more efficient than vessels at trapping gas bubbles, which has important consequences in relation to the restoration of water to empty (*cavitated*) xylem elements.

Only the sapwood actually conducts water through stems and branches (Fig. 2.8). Heartwood, which forms internally from sapwood, has a majority of cells filled with gas or impermeable metabolic products. Water columns in the capillaries of sapwood have great cohesiveness as a result of strong surface tensions associated with the way that water molecules are hydrogen bonded (Jones, 1992). The strong cohesion of water molecules to one another allows them to be pulled upward through the stem to wet surfaces of leaf cell walls from which water is transpired through stomata, or more slowly through the leaf cuticle.

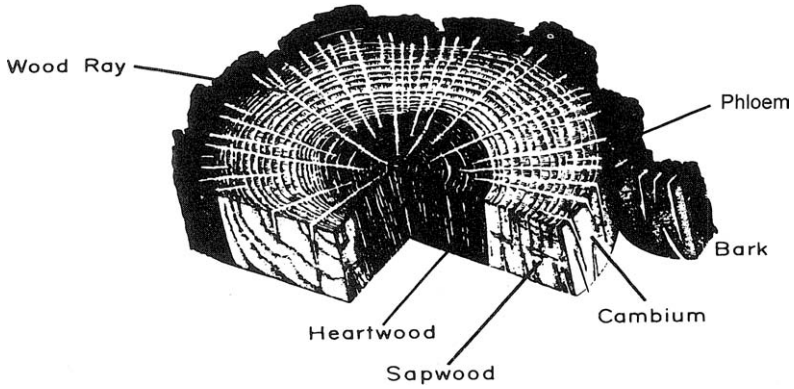

FIGURE 2.8. A section of an oak stem shows various anatomical components. The outer bark protects the cambium where cell divisions occur, producing wood inward and phloem outward. Water and nutrients are conducted from the roots to the leaves via conducting elements in the sapwood. Large wood rays transverse the sapwood and inner heartwood. The ray cells are alive in the sapwood but no longer function in the heartwood. (From Raven *et al.,* 1981.)

The movement of water through trees is dependent on the difference in the energy state of water from point to point in the system (Fig. 2.1). The energy state of water is usually expressed as the potential (Ψ) relative to pure, free water with units of pressure (megapascals), equivalent to a force per unit area ($1\,\text{MPa} = 1.02 \times 10^5\,\text{kg}\,\text{m}^{-2}$). Flow is always in the direction of more negative Ψ. Water potential in plants may be separated into four components:

$$\Psi = \Psi_p + \Psi_s + \Psi_m + \Psi_g \tag{2.12}$$

where Ψ_p, Ψ_s, Ψ_m, and Ψ_g, respectively, are related to pressure, solute, matric, and gravitational forces. The pressure component (Ψ_p) represents the difference in hydrostatic pressure from one cell to another, and it is the only component which can be positive or negative. The solute potential (Ψ_s) represents the contribution of dissolved sugars and salts. The matric potential (Ψ_m) results from small negative forces at the surface of solids such as cell walls or soil particles. The gravitational component (Ψ_g) increases with height above ground at $0.01\,\text{MPa}\,\text{m}^{-1}$.

As molecules of water are vaporized and diffuse from leaves, tension in the sapwood water columns increases. Living cells possess semipermeable membranes and can accumulate solutes which lower the water potential within cells, increasing the potential gradient and causing water to be extracted from the vascular system. As a result of accumulating solutes and by changes in cell wall permeability, living cells remain relatively turgid through most droughts. The high concentration of solutes in the thin layer of *phloem* located between the cell-dividing *cambium* and bark (Fig. 2.8) can create a reverse flow from the top of a tree downward toward growing roots or other organs where sugar and other metabolites become concentrated.

In nontranspiring small trees, with water readily available to roots, the xylem potential of leaves is about $-0.2\,\text{MPa}$. Transpiration causes tension in the water columns, and Ψ

falls rapidly to −1.5 MPa or below. The water potential gradient, $\Delta\Psi$, in this case, represents the difference between transpiring and nontranspiring conditions. Under drought stress, predawn water potentials in nontranspiring trees may fall well below −1.5 MPa, occasionally to −8 MPa (Tyree and Dixon, 1986), but $\Delta\Psi$ values are small under such conditions because stomata remain closed.

Predawn Ψ status, which usually represents conditions with zero transpiration, is an important reference base for interpreting and modeling water flow through trees. Leaf water potential is usually measured with a pressure chamber using twigs or single leaves (Scholander *et al.,* 1965; Ritchie and Hinckley, 1975). Assuming a steady-state situation, the relationship between hydraulic conductivity (K_h) of the xylem and the tension on the water column can be quantified using an analog of Ohm's law:

$$K_h = F\Delta z/(\Psi_{soil} - \Psi_{leaf}) \tag{2.13}$$

where F is the flux of water ($kg\,s^{-1}$) and ($\Psi_{soil} - \Psi_{leaf}$) is the water potential gradient ($\Delta\Psi$) between the leaf and soil, per unit distance (Δz, m) the water travels. Ψ_{leaf} measured under nontranspiring conditions is often substituted for Ψ_{soil}. The hydraulic conductivity (K_h, $kg\,m^{-1}\,s^{-1}\,MPa^{-1}$) is independent of the diameter of the stem at any particular point. Specific conductivity (K_s, $kg\,m^{-1}\,s^{-1}\,MPa^{-1}$) of a stem (or branch) is K_h normalized by the area of conducting tissue (m^2) in the cross section and is a measure of porosity. Leaf-specific conductivity (LSC, $kg\,m^{-1}\,s^{-1}\,MPa^{-1}$) is K_h normalized by the leaf area (m^2) distal to the stem and is the best general reference for comparing the efficiency of one species with another in conducting water to transpiring surfaces (Tyree and Ewers, 1991).

Wood permeability may be determined in the laboratory by measuring the flow of water under constant pressure through samples of specified length and cross-sectional area. From such measurements, it has been demonstrated that the outer zone of sapwood may have a permeability as much as 10 times that of the inner zone (Comstock, 1965). Also, progressing up the stem to the base of the live crown, sapwood permeability tends to increase. The significance of these trends is that hydraulic conductivity (K_h), represented by the product of the average permeability and sapwood area, remains constant from the base of the stem to the live crown, although the total cross-sectional area of sapwood may be reduced by more than threefold (Shelburne and Hedden, 1996).

From such analyses of wood permeability, we find that species well adapted to their environment exhibit significantly higher wood permeability and conductances than less well adapted species, or those situated in an unfavorable competitive position relative to neighboring individuals (Sellin, 1993; Shelburne and Hedden, 1996). Once trees reach maximum height, the total resistance to water flow, when sapwood is saturated, tends to approach a common value (Pothier *et al.,* 1989). Much effort has gone into analyzing anatomical differences in wood structure, with wood density an obviously important variable, but the dominant control on stem conductance appears to be the fraction of sapwood that remains in a saturated state (Waring and Running, 1978; Shelburne and Hedden, 1996).

Hydraulic properties of various structural components can also be determined in the field or laboratory by sequentially cutting off portions of a tree under water and providing the remaining system free access to a monitored water reservoir. From such analyses, the branches and twigs have been found to offer the highest resistance to flow, and, being at

the end of the vascular system, they are more likely to suffer permanent damage from cavitation than the main stem (Zimmermann, 1978; Tyree *et al.,* 1994).

B. Seasonal Variation in Water Content and Hydraulic Conductivity

In transpiring plants, the water stored in tissues is not in steady state, as assumed by Ohm's law. The tissues in a plant may be considered as a number of alternative sources of water linked in parallel with each other and the soil. As water is lost through transpiration, the flows out of storage at any one time and their relative phasing depend on the resistances between the stores and the xylem, the capacity of the stores, and the relationship between Ψ_{leaf} and tissue moisture characteristics (see Landsberg, 1986a). Initially, water will move out of storage from the leaves; however, this source is small (Whitehead and Jarvis, 1981), and the potential will quickly drop, shifting the main source of supply progressively lower down the plant. The extraction of water from branches and stems may contribute up to 1–2 mm day^{-1}, and it explains why measurements of sap flow made at the base of trees, by introducing metal probes and measuring the velocity of a heat pulse upward, show that flow there often lags 1–2 hr behind measured rates of transpiration (Fig. 2.9; see Granier *et al.,* 1996, for comparison of four related methods). Extraction of water from the sapwood appears to account for the majority of water supplied to buffer the difference between the recorded flow in the stem and losses from the canopy (Waring *et al.,* 1980; Tognetti *et al.,* 1996).

As a consequence of emptying the larger diameter xylem elements first, the hydraulic conductivity of stem and branches is reduced exponentially as the relative water content of sapwood decreases. This in turn causes stomatal closure at progressively lower vapor pressure deficits (Waring and Running, 1978; Sperry and Pockman, 1993; Lo Gullo *et al.,* 1995). Wet temperate species begin to experience cavitation at moderate water potentials between −0.8 and −1.5 MPa, as documented by the recording of acoustic emissions from tree stems (Sandford and Grace, 1985; Sperry *et al.,* 1988; Sperry and Pockman,

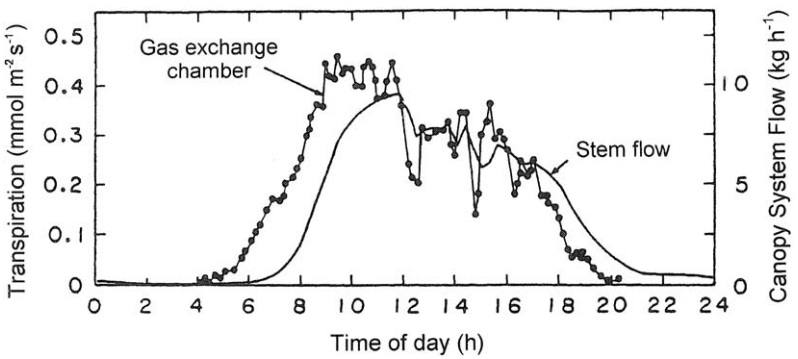

FIGURE 2.9. Water uptake, tracked by measuring the velocity of a heat pulse up the stem, may lag 20–30% behind cuvette measurements of water transpired through leaf stomata during the day. Recharge of the reservoirs in sapwood and other tissues occurs as water uptake continues through the night. (After Schulze *et al.,* 1987. © 1987 American Institute of Biological Sciences.)

1993; Jackson *et al.,* 1995). Species adapted to harsher environments, such as *Juniperus,* do not experience cavitation until water potentials fall below −3.5 MPa and still maintain some functional xylem at potentials below −8.8 MPa (Tyree and Dixon, 1986).

One practical way of assessing whether major seasonal changes in hydraulic conductance occur that could affect predictions of stomatal conductance (g_s) is to extract small wood core samples of known volume from near the base of trees and determine the relative water content (RWC) by measuring wood density and moisture content, assuming that cell wall constituents have a constant density of 1530 kg m^{-3} (Siau, 1971). From such an analysis, an old-growth Douglas-fir forest subjected to a long period of summer drought was shown to experience major seasonal changes in RWC, and recovery to a fully saturated state required many months following the commencement of precipitation (Waring and Running, 1978; Fig. 2.10).

Conifers with a high proportion of sapwood in their stems (such as *Pinus*) or species that accumulate large biomass (such as Douglas-fir) may store more than 200 Mg H_2O ha^{-1}, equivalent to 20 mm in sapwood (Waring and Running, 1978; Waring *et al.,* 1979). The mechanisms by which cavitated cells in xylem refill are not fully understood. Mobilization of sugars in roots on some angiosperms can create root pressure and force water into previously cavitated xylem (Sperry *et al.,* 1988). For tall conifers, other processes must

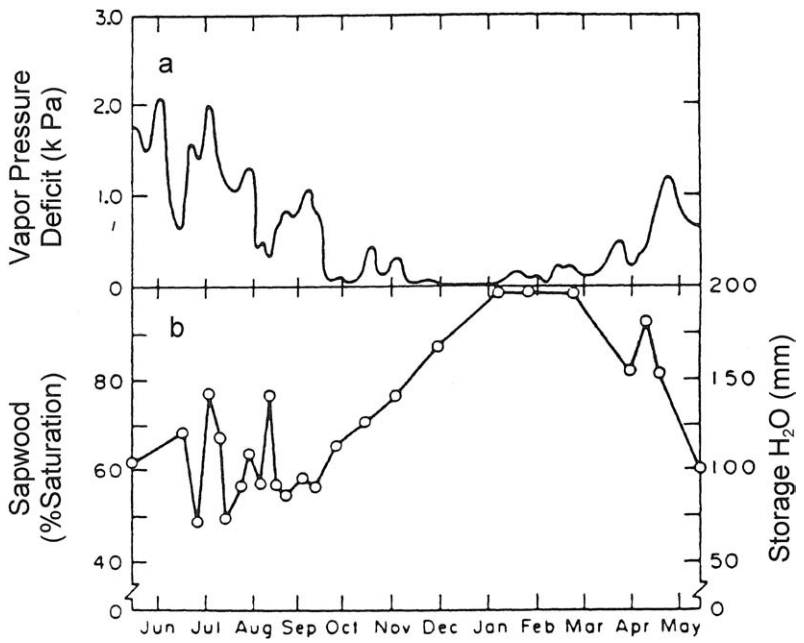

FIGURE 2.10. Withdrawal of water from the sapwood of a 500-year-old Douglas-fir forest growing in the Pacific Northwest begins in March at the start of the growing season, and stored water reaches its lowest level during summer drought periods. Full recharge of the sapwood occurs in the winter when rainfall is high. Over the course of the year, the sapwood water reservoir was depleted by 125 mm and its relative water content reduced from 100 to 50%. (From Waring and Running, 1978.)

operate, some of which appear dependent on dew or periods of high rainfall to minimize internal water potential gradients (Sobrado *et al.,* 1992; Edwards *et al.,* 1994; Boucher *et al.,* 1995; Magnani and Borghetti, 1995).

Trees adapted to harsh environments, where freezing and drought commonly occur, support less leaf area per unit of sapwood area (measured usually at 1.3 m and extrapolated, with knowledge of stem taper, to the base of the live crown) than species or varieties adapted to less stressful conditions. For example, ponderosa pine and Douglas-fir native to Oregon support almost twice the leaf area per unit of sapwood compared with related forms growing in the more continental state of Montana (Table 2.3). Adjustments between leaf area and sapwood area demonstrate a structural property of trees that helps maintain functional xylem and results in similar values of specific leaf conductivity.

TABLE 2.3
Ratio of Projected Leaf Area to Sapwood Cross-sectional Area at Breast Height for Selected Tree Species

Tree species	Leaf area/sapwood area, ratio, m^2/m^2	Reference
Conifers		
Abies balsamea	7100	Coyea and Margolis (1992)
Ahies lasiocarpa	7500	Kaufmann and Troendle (1981)
Abies procera	2700	Grier and Waring (1974)
Picea engelmannii	3500	Waring *et al.* (1982)
Pinus contorta	1500	Waring *et al.* (1982)
Pinus ponderosa (Montana)	1400	Gower *et al.* (1993)
Pinus ponderosa (Oregon)	2500	Waring *et al.* (1982)
Pinus sylvestris (England)	800	Mencuccini and Grace (1995)
Pinus sylvestris (Scotland)	1700	Mencuccini and Grace (1995)
Pseudotsuga menziesii var. *glauca* (Colorado)	2500	Snell and Brown (1978)
Pseudotsuga menziesii var. *menziessi* (W. Oregon)	5400	Waring *et al.* (1982)
Tsuga heterophylla	4600	Waring *et al.* (1982)
Tsuga mertensiana	1600	Waring *et al.* (1982)
Hardwoods		
Acer macrophyllum	2100	Waring *et al.* (1982)
Castanopsis chrysophylla	4600	Waring *et al.* (1982)
Eucalyptus regnans	3100	Vertessy *et al.* (1995)
Nothofagus solanderi (subalpine)	700	Benecke and Nordmeyer (1982)
Nothofagus solanderi (montane)	1200	Benecke and Nordmeyer (1982)
Populus tremuloides	1000	Kaufmann and Troendle (1981)
Quercus alba	4000	Rogers and Hinckley (1979)
Tectona grandis	6500	Whitehead *et al.* (1981)

C. Carbon Isotope Discrimination of Hydraulic Limitations on Stomatal Conductance

Carbon dioxide in the air diffuses into leaves through stomata and is incorporated through photosynthesis into biomass (Chapter 3). In the atmosphere, two stable isotopic forms, carbon-13 (^{13}C) and carbon-12 (^{12}C), exist in a ratio of about 1 : 84 in today's fossil fuel-enriched atmosphere. During photosynthesis, plants selectively favor the lighter and more abundant form (^{12}C) over the heavier isotope, but the degree of discrimination is dependent to a large extent on the stomatal conductance. Discrimination (Δ) is defined as the difference in relative molar abundance of $^{13}C/^{12}C$ in the atmosphere compared to that in photosynthetic products. Because the normalized ratios of heavy to lighter forms of stable isotopes are so small, isotopic composition is conventionally expressed as parts per thousand (‰) in reference to deviations (δ) from the abundance ratio in a nonvarying reference standard, which, in the case of carbon, is a carbonate rock, from a Pee Dee Belemnite formation in South Carolina with a $^{13}C/^{12}C$ ratio of 0.01124. Deviations are calculated as

$$\delta^{13}C‰ = \{[(^{13}C/^{12}C)_{sample}/(^{13}C/^{12}C)_{standard}] - 1\}1000. \quad (2.14)$$

As CO_2 diffuses into leaves through stomata, ^{13}C moves more slowly than ^{12}C and is discriminated against by 4.4‰. An additional discrimination of 30‰ against ^{13}C occurs in carbon fixation. When stomatal conductance is reduced, photosynthesis continues, and the internal concentration of CO_2 falls so that a greater proportion of the intercellular $^{13}CO_2$ reacts with the carboxylating enzyme. As a result, an indirect measure of the restrictions on stomatal conductance may be obtained by analyzing, with a mass spectrometer, the carbon isotopic composition of leaves or wood samples.

In New Zealand, the importance of branch length as a major factor limiting stomatal conductance was confirmed by comparing the isotopic composition of foliage situated at the ends of pine branches of varying length but at similar height above the ground (Fig. 2.11). In a less maritime climate than New Zealand, where the relative water content in branch wood does not remain near saturation, $\delta^{13}C$ values measured in foliage at the end of branches still reflect the leaf-specific conductivity (Panek, 1996). As trees approach maximum height, hydraulic limitations increase, which reduces g_{max} from values typically obtained on younger trees (Yoder *et al.,* 1994). The $\delta^{13}C$ analysis of foliage or wood samples quantifies the extent to which age and inherently stressful site conditions need to be taken into account in modeling transpiration and photosynthesis.

D. Soil Limitations on the Flow of Water through Plants and Stomatal Conductance

All the water transpired by vegetation is taken up by roots from the soil. The amount of water stored in soils and available to roots is among the most difficult but critical measurements to obtain. Forest soils are generally not as uniform as agricultural fields, and rooting depths of trees may vary from 0.1 to >10 m. In this section we describe how estimates of soil water storage are obtained, what limitations are placed on water extraction by roots, and what implications these limitations have on restricting stomatal conductance.

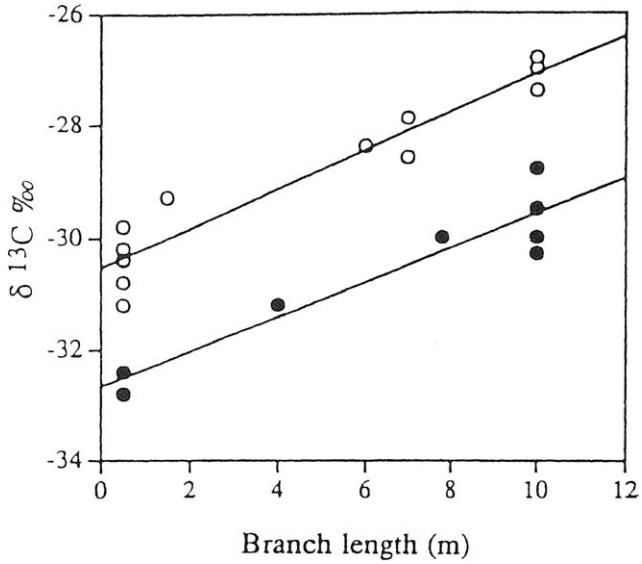

FIGURE 2.11. The normalized ratio of carbon-13 to carbon-12 isotopes ($\delta^{13}C$) from foliage of *Pinus radiata* becomes less negative, which indicates relatively more enrichment in the heavier isotope carbon-13, with increasing branch length. Branches on more exposed aspects (○) show proportionally more enrichment of carbon-13 than those less exposed to direct solar radiation (●). The $\delta^{13}C$ isotopic ratios reflect time-integrated differences in hydraulic conductivity of branches. As stomata are forced to close, the internal concentration of CO_2 decreases, increasing the proportion of the heavier isotope (^{13}C), which is normally discriminated against by photosynthetic enzymes, that becomes incorporated in photosynthetic products. (After Waring and Silvester, 1994.)

Water uptake by roots depends on the absorbing surface area, membrane permeability, and the $\Delta\Psi$ between roots and soil (Landsberg and Fowkes, 1978; Landsberg and McMurtrie, 1984). The soil water potential (Ψ_{soil}) is the sum of gravitational, pressure, solute, and matric potentials. In most forest soils, salt concentrations are low, and thus the matric potential is the most important component. As soils dry, the energy required to extract water increases quickly as the water most freely available in large pores is depleted first.

The volumetric water content θ is the fraction of soil volume consisting of water and is calculated as

$$\theta = (m_{water}/m_{soil})\rho_{soil}/\rho_{water} \tag{2.15}$$

where m_{water}/m_{soil} is the mass of water per unit mass of soil, and ρ_{soil}/ρ_{water} is the ratio of the soil bulk density to the density of water ($1000\,kg\,m^{-3}$). The volume of water in the rooting zone would be equivalent to the product of θ and the rooting depth. Soil porosity is the ratio of the volume of pore space per unit volume of soil; when $\theta = 1.0$, all pore spaces are filled and the soil is saturated. In most cases, soil porosity is between 0.3 and 0.6, depending on the bulk density, texture, and content of organic matter and rock.

Soil water can be separated into a number of functional categories: a rapidly draining component associated with pores $>50\,\mu m$ in diameter, a fraction available to plant roots

that is held in pores between 0.2 and 50 μm (at Ψ_{soil} between about −0.01 and −1.5 MPa), and an unavailable fraction in pores <0.2 μm that is only lost through evaporation near the soil surface (Fig. 2.12). A sandy soil with a bulk density of 1200 kg m^{-3} is shown (at the intercept on the *x* axis) to have a porosity only slightly less than loam or clay soils (0.45–0.48) with similar bulk densities. Sandy soils, however, have large and uniform pores between particles, compared to smaller and more variable pore-size distributions characteristic of most finer textured soils. As a result, the moisture-retention curves in relation to soil water potentials differ with soil texture. The maximum storage of water available (θ) for plants in a cubic meter of soil with textures shown in Fig. 2.12 is as follows: sand, 0.12 − 0.05 = 0.07 m^3; loam, 0.38 − 0.14 = 0.24 m^3; clay, 0.46 − 0.31 = 0.15 m^3.

Following recharge of a soil profile, plants normally extract water first from the upper soil horizons where root density is highest. Water is then progressively extracted from lower horizons, unless precipitation occurs (Nnyamah and Black, 1977; Hinckley *et al.,* 1981; Talsma and Gardner, 1986). Species exploit the soil to differing extents. Shallowly rooted trees or shrubs exhibit more negative water potentials than more deeply rooted associates under droughty conditions (Hinckley *et al.,* 1983). In both arid and tropical wet zones, trees are buffered against drought by root systems that extend >10 m below the surface (Doley, 1981; Nepstad *et al.,* 1994). Although detailed models exist for calculating

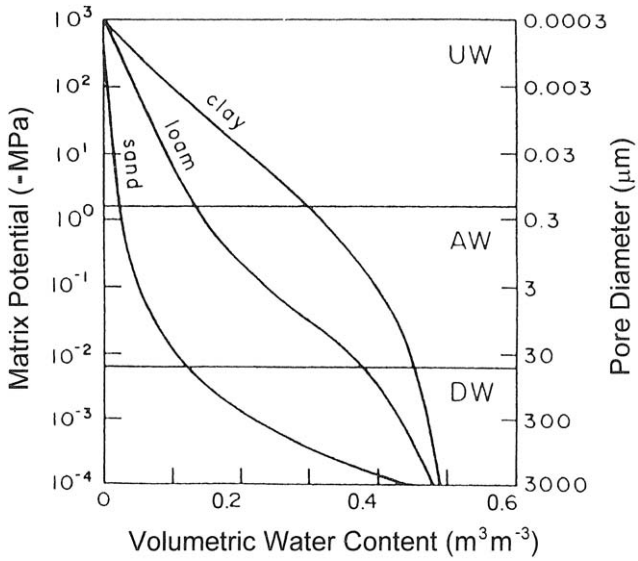

FIGURE 2.12. Water storage capacity of soils varies with texture, reflecting pore size distribution. Water in pores below 0.2 μm diameter is unavailable to roots (UW), being held at soil matrix potentials at or below −1.5 MPa. Available water (AW) is held in pores in the range from 0.2 to 50 μm, equivalent to matrix potentials between about −0.01 and −1.5 MPa. As pore size increases above 50 μm, capillary forces are unable to hold water, and it drains rapidly (DW zone in the graph). Soils of similar density (here about 1200 kg m^{-3}) and porosity (θ between 0.43 and 0.48) vary in the volume of available water per cubic meter of soil from θ = 0.07 m^3 in the sand to 0.24 m^3 in the loam. (After Ulrich *et al.,* in *Dynamic Properties of Forest Ecosystems,* 1981, courtesy of Cambridge University Press.)

water uptake from different soil horizons as a function of soil properties and root density (see Landsberg, 1986a), data requirements are too high for inclusion in most ecosystem models. These models generally include only an estimate of maximum rooting depth and assume that roots are equally distributed or, alternatively, concentrated mostly in the upper soil horizon.

Depending on soil texture and root distribution, between 45 and 75% of the available water can usually be extracted from the rooting zone before transpiration is reduced below maximum rates and plants exhibit a significant reduction in predawn Ψ (Fahey and Young, 1984; Dunin *et al.,* 1985; Fig. 2.13a). Small additions of water following a single storm may permit a full recovery to minimum predawn Ψ while most of the soil profile remains dry. Generally, the maximum opening of stomata during the day decreases exponentially as predawn Ψ falls (Running, 1976; Schulze, 1986; Reich and Hinckley, 1989; Ni and Pallardy, 1991; Fig. 2.13b).

Water uptake by roots is affected by soil temperature and oxygen levels, as well as by limited availability of water in dry soils. Low root temperatures limit water uptake because the viscosity of water near freezing is approximately twice that at 25°C (Nobel, 1991). Plants adapted to warm or to cold climates differ in their root permeabilities as a result of varying lipid–protein ratios in root membranes. As a result, water uptake by the roots of a subalpine species such as *Pinus contorta* shows sensitivity to temperatures only below 5°C (Running and Reid, 1980), whereas for a maritime species such as *Pinus radiata,* water uptake is inhibited until soil temperatures exceed 15°C (Kaufmann, 1977). In the southern hemisphere, where an ancient subtropical tree flora has evolved and now survives in a temperate climate, root resistance to water uptake at temperatures below 10°C appear to limit stomatal conductance more than for typical temperate forest species (Hawkins and Sweet, 1989; Waring and Winner, 1996).

As soils drain, the oxygen levels increase as more void spaces become air filled. At saturation, soils have no unfilled void spaces, and oxygen in the water is rapidly depleted by respiration of roots and microorganisms. Some species are resistant to flooding, such as *Fraxinus pennsylvanica, Nyssa aquatica,* and *Taxodium distichum,* and continue to grow roots when inundated (Hook *et al.,* 1970; Dickson and Broyer, 1972; Keeley, 1979). The ability to grow under such conditions indicates the passage of oxygen from above the water level, aerating the rooting zone. Upland plants subjected to flooding rarely exhibit water stress, probably because their stomata remain closed (Pereira and Kozlowski, 1977; Kozlowski and Pallardy, 1979) as a result of an altered hormone balance (Rinne *et al.,* 1992; Jackson, 1994). Compacted soils, whether wet or dry, offer limited air spaces for oxygen to diffuse to roots. As the bulk density of soils increases, average pore size decreases. As a result, roots are unable to penetrate soils with soil bulk densities much above $1500\,kg\,m^{-3}$ (Heilman, 1981; Tworkoski *et al.,* 1983).

E. Indirect Approaches to Defining Water Available to Plant Roots

The water available in the soil rooting zone (θ, mm) is one of the most difficult variables to quantify. Given good estimates of daily transpiration, soil water storage capacities may be indirectly estimated by adjusting the value of available θ to about 30% of the storage capacity, which corresponds to when predawn Ψ first begins to fall below its maximum

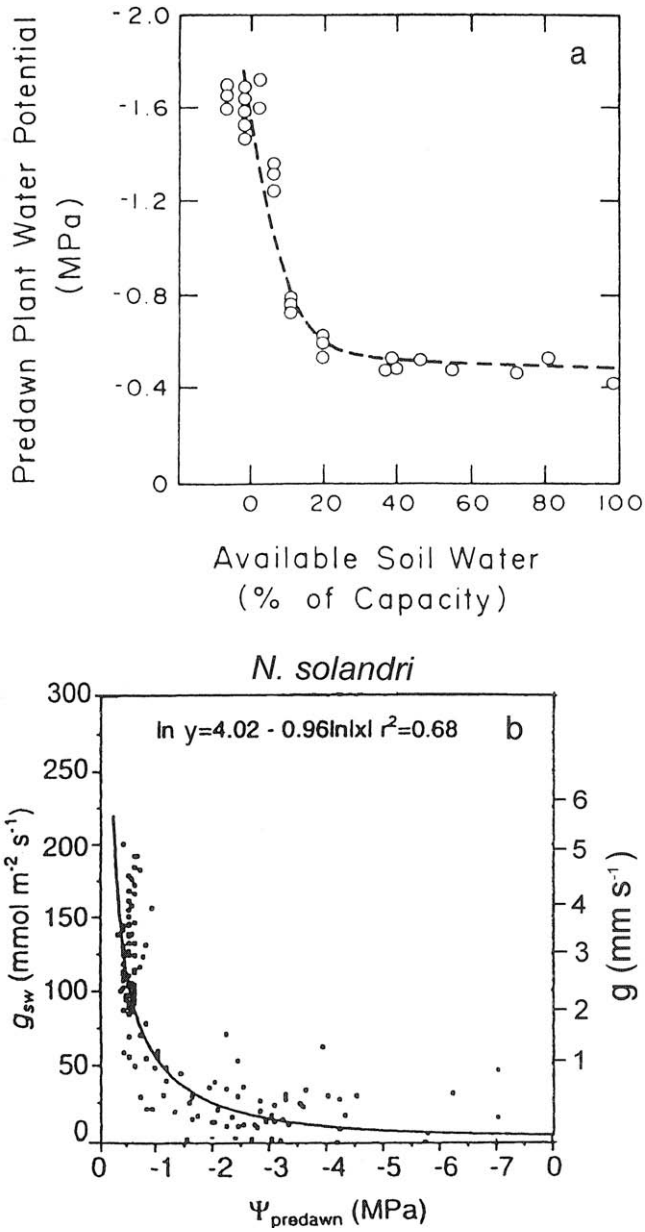

FIGURE 2.13. (a) Until more than three-quarters of the available water held between −0.01 and −1.5 MPa is depleted from the rooting zone, a pine stand exhibits a constant predawn water potential of −0.5 MPa. As the remaining available water is withdrawn from the soil, predawn Ψ falls rapidly to below −1.5 MPa. (After "Water potential in red pine: Soil moisture, evapotranspiration, crown position" by E. Sucoff, *Ecology,* 1972, **53,** 681–686. Copyright © 1972 by the Ecological Society of America. Reprinted by permission.) (b) Maximum daily leaf stomatal conductance (g_s in two alternative units) for *Nothofagus solandri,* native to New Zealand, shows an exponential decrease as predawn water potential ($\Psi_{predawn}$) falls. (After Sun *et al.,* 1995.)

(Fig. 2.13a). When roots can tap groundwater or seeps, transpiration will not be limited by the water holding properties of the soil. Other methods are required to assess whether trees have access to such sources, although measurement of predawn Ψ will provide indirect evidence by showing values are maintained near maximum independent of the calculated soil–water balance.

Stable isotopes of oxygen ($^{18}O/^{16}O$) and hydrogen ($^{2}H/^{1}H$ or D/H) in the sap stream and cellulose of annual growth rings provide a means of distinguishing the extent to which plants tap groundwater sources (Ehleringer and Dawson, 1992). Isotopic differences between groundwater and surface sources result from not only atmospheric circulation patterns that distribute precipitation but also isotopic fractionations taking place during evaporation and condensation. The source of most atmospheric water vapor is tropical oceans. As water evaporates, the heavier isotopes are discriminated against so that water vapor, in relation to seawater (the standard), has a more negative $\delta^{18}O$ and δD. As the vapor moves into higher latitudes and cools, rain or snow is condensed from the air mass. Condensation is a fractionating process that removes the heavier isotopes and leaves the lighter behind as vapor. Thus, as atmospheric water vapor moves up in latitude or in elevation, its isotopic signatures become progressively lighter, which is reflected in the composition of the precipitation and results in a good correlation with mean annual temperature (Fig. 2.14).

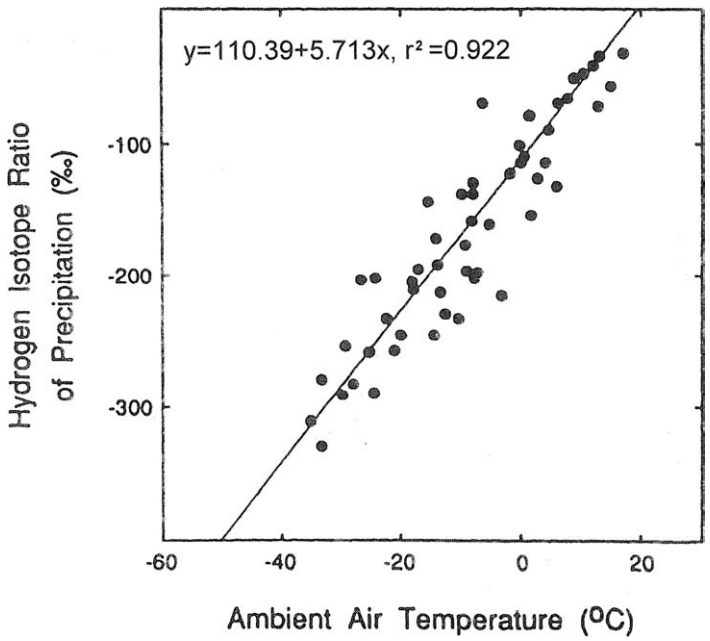

FIGURE 2.14. The hydrogen isotopic ratio in precipitation decreases linearly in association with ambient air temperature, as does that of $\delta^{18}O$, which is functionally related: $\delta^{18}O = (\delta D/8) - 10‰$. (After Ehleringer and Dawson, 1992.)

Precipitation that falls during winter months, when temperatures are low, is less likely to be evaporated and therefore contributes most to the groundwater (or seepage water derived from higher elevations). During the summer, if plant roots tap the water table, the water transferred from the deepest plant roots may diffuse out from other roots occupying very dry surface soils. In arid environments shallow-rooted plants may thus gain access to water far below their rooting depth (Fig. 2.15a). Even in areas where summer precipitation is common, plants that tap deep sources of water, including the groundwater, show much more negative δD values in their xylem sap and wood cellulose than those that draw on only surface horizons and therefore mirror the isotopic composition of summer precipitation (White *et al.,* 1985; Fig. 2.15b).

In summary, the upper limit to flow of liquid water through trees is set by structural features: the amount of leaves, tree height, branch length, xylem anatomy, and root development. Low soil temperatures, flooding, drought, and other factors further limit flow. In trees, sapwood and deep roots provide buffers against water deficits, but as wood and soil reservoirs are exhausted, reductions in leaf area and plant (and soil) hydraulic conductances occur. Measurements of predawn plant water potential and wood relative water contents provide functional measures of drought and seasonal limitations on estimates of maximum stomatal conductance. The stable isotopic composition of carbon, found in leaves and wood, provides an integrated signal of hydraulic limitations on water uptake and flow through stems and branches. Stable isotopes in water, when analyzed in the xylem sap and wood cellulose, provide a way of determining the relative contributions of subsoil and groundwater to transpiration.

IV. WATER STORAGE AND LOSSES FROM SNOW

A. Interception, Accumulation, and Energy Exchange Processes

To complete the story of surface storage and losses of water, we must consider water in its frozen state as snow or ice. As mentioned previously, snow accumulates on the canopy in proportion to leaf area index, but most is shed or falls directly to the soil surface where it may accumulate to great depths. Fresh snow contains between 6 and 35% water by volume. The density of a snowpack increases to a maximum when snowmelt begins, at which time the water content per cubic meter is uniform and the temperature throughout the pack is isothermal at 0°C.

With the exception of freezing of liquid water within the pack and conduction of heat from the ground, all components of the energy balance can be treated as within a thin surface layer of snow (Anderson, 1968). The surface temperature and albedo of snow (Table 2.1) are two key properties needed to calculate energy exchange and to determine whether snow is converted directly to water vapor (*sublimation*) or melts. When warm, moist air condenses on the cold surface of snow, heat as well as moisture is added to the snowpack (2501 kJ kg^{-1} at 0°C). If the gradient is reversed, moisture and heat are lost. If the snow surface is below 0°C, the latent heat of sublimation required to turn snow directly to water vapor (355 kJ kg^{-1}) must be added. Latent heat transfer can be important in areas where warm, moist, turbulent air is advected over snowpacks, because 1 mm of condensate can produce about 7.5 mm of melt (Anderson, 1968).

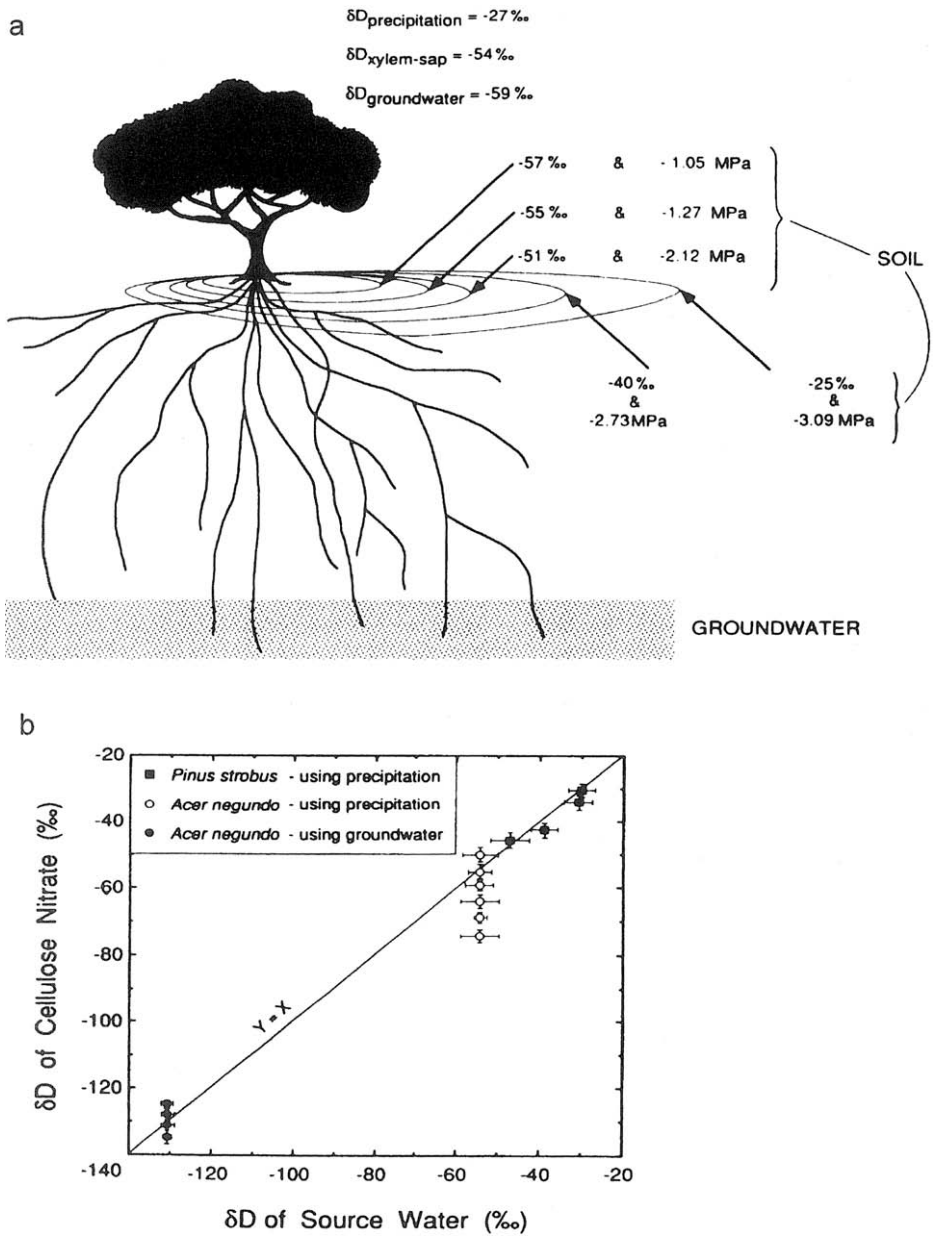

FIGURE 2.15. (a) The hydrogen isotopic composition of xylem sap (δD‰) indicates that an isolated tree (*Acer saccharum*) obtains >90% of its water during a summer drought from snowmelt-enriched groundwater. Some water leaks from the tree's roots into the upper soil horizon (0–35 cm), which explains the decreasing water potential gradient (MPa) measured up to 5 m from the tree. (b) Cellulose nitrate δD compares well with that of source water for white pine (*Pinus strobus*) growing in New York State (■) and for shallow- (○) and deep-rooted (●) boxelder (*Acer negundo*) growing near a stream in Utah. (After Dawson, 1993.)

Rain is warmer than the snowpack, and hence there is a transfer of heat from rain to the snowpack. Knowing the specific heat of water ($4.18\,kJ\,kg^{-1}\,K^{-1}$), the heat added is easily calculated from the amount of precipitation and air (rain) temperature. Because the latent heat of fusion is only $334\,kJ\,kg^{-1}$, the temperature of the snowpack is not much affected by the process of freezing water. For example, 4 mm of rain at 20°C must be added to a "ripe" snowpack (at 0°C and maximum water-holding capacity) to produce 1 mm of melt. When the snowpack is below freezing, however, rain adds its small heat content and gives up the latent heat of fusion as it freezes within the pack. This may quickly bring a cold snowpack to a uniform (isothermal) temperature of 0°C, ripe for melting. When melt occurs, water percolates down where it may refreeze. Melt is held until the water-holding capacity of the pack is exceeded ($350\,kg\,m^{-3}$).

B. Modeling Snow in the Hydrologic Balance

Coughlan and Running (1997a) developed a computer simulation model of snow accumulation and melt that requires a minimum of meteorological information (daily precipitation, maximum and minimum temperature) and properties of the site (elevation, slope, aspect, and LAI). With these data, they generated a water and energy balance to calculate daily snowfall, evaporation and sublimation, storage water in the pack, and melt at 10 sites scattered across the western United States. Soils were assumed to be at saturation to simplify calculations further (see Section V). The model accounts for changes in albedo as snow ages and applies the Beer–Lambert law to calculate short-wave radiation penetration through canopies to permit calculation of snow melt and other processes beneath a forest canopy.

Snow pillows situated on weighing lysimeters provided independent estimates of snow water content and snow melt over a 3-year period. Model predictions were in close agreement with measured values of water content of the snowpack (Fig. 2.16a) and spring melt for most sites (Fig. 2.16b). Sensitivity analyses confirmed the general importance of LAI in influencing snow accumulation and melt. Topographic variables became particularly important at higher elevation sites in early spring when sunny weather predominates and large differences in radiation occur between north and south aspects. In early summer, when solar zenith angles are higher, aspect has much less influence on melt.

The amount of water stored in a snowpack may exceed that stored in soils by some orders of magnitude, but most is not available to plants. When melt occurs, the majority of water flows through saturated soil into groundwater and streams. The presence of snow may, on the other hand, significantly delay the initiation of growth by keeping soil and root temperatures near freezing. Forest cover has a major influence on snow hydrology.

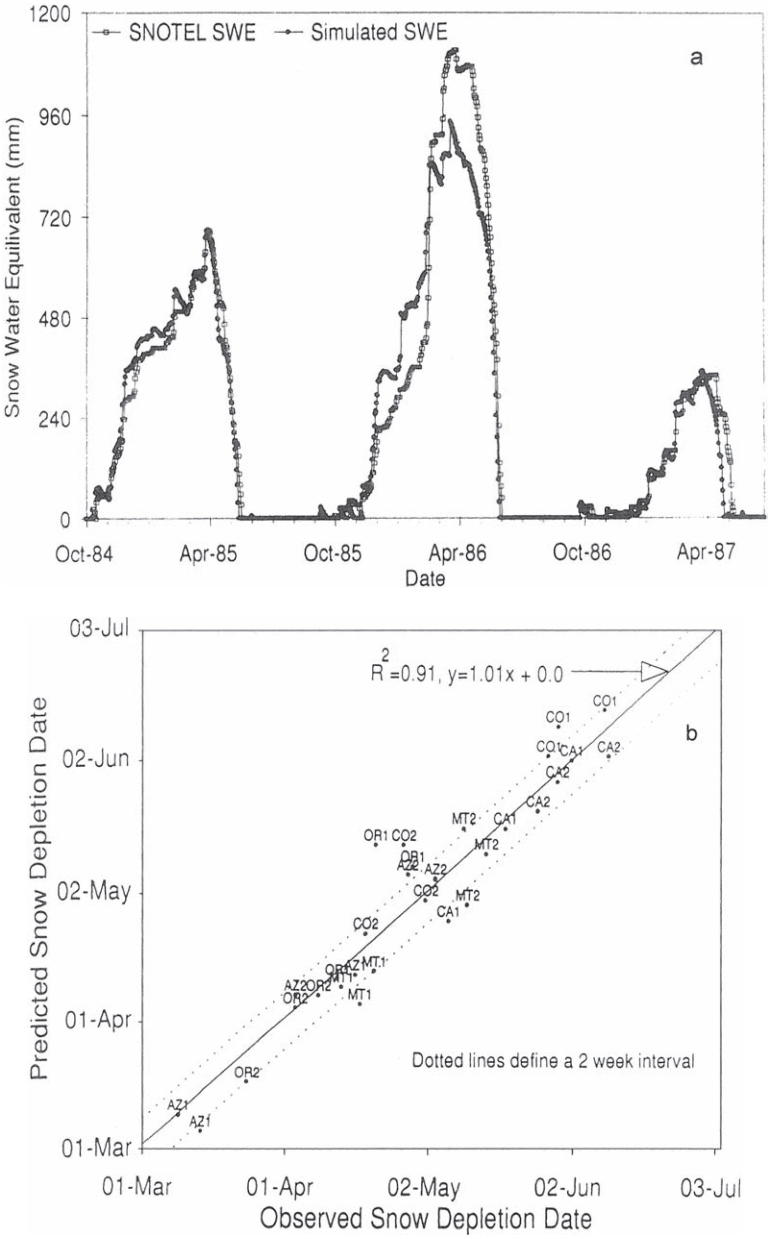

FIGURE 2.16. (a) Changes in snow water content measured on a snow pillow compared well with FOREST-BGC modeled daily predictions over 3 years. (b) The dates of complete snowmelt were predicted by a snow hydrology model over a 3-year period at 10 locations in the western United States (represented by abbreviations of the states). In general, model predictions were in good agreement with observed values. (After *Landscape Ecology,* Volume 12, J. C. Coughlan and S. W. Running, "Regional ecosystem simulation: A general model for simulating snow accumulation and melt in mountainous terrain," pp. 119–136, 1997, with kind permission of Elsevier Science–NL, Sara Burgerhartstraat 25, 1055 KV Amsterdam, The Netherlands.)

An evergreen canopy absorbs almost all short-wave radiation, while a deciduous canopy with snow on the ground reflects most of the radiation upward. Interception losses are highest from dense evergreen canopies; however, losses from the snowpack on the ground are minimal, and melting may be long delayed compared to forests with more open or deciduous canopies. No additional meteorological variables or structural description of canopies, beyond those required to estimate evaporation from wet surfaces, are required to model snow hydrology, an important point for developing generalized ecosystem models.

V. WATER FLOW ACROSS AND THROUGH SOIL

A. Surface Runoff

In this section we review the major processes that control the movement of water after it reaches the ground. Once water reaches the soil surface, the rate and direction of flow are determined by soil and topography. Surface runoff may sweep litter and pollutants directly into streams, but this rarely occurs on fully forested watersheds. In forests, natural channels created by roots, burrowing animals, and drying cracks are important in permitting water to flow rapidly into streams without first wetting all of the soil. The kind of vegetation and its history of disturbance also affect the infiltration properties of surface litter and soil. The rate at which throughfall reaches the soil is a function of the kind of litter as well as the amount. Certain soil types are known to be *hydrophobic* when dry and to absorb water very slowly (DeBano and Rice, 1973); these conditions are often enhanced following fire through transfer of dissolved residues into the surface soil (Shahlaee *et al.,* 1991; Everett *et al.,* 1995).

B. Infiltration and Percolation

Once water reaches the soil surface, whether it runs off or enters the soil depends on the rate of delivery and infiltration capacity of the soil. The maximum infiltration capacity of soils is largely determined by pore size distribution, and bulk density. The two determinants of soil water movement are the driving force of the hydraulic potential gradient and the soil's hydraulic conductivity. The hydraulic pressure potential gradient ($\Delta\Psi/\Delta z$) is the difference between the gravitational potential (Ψ_g, $+0.01\,\mathrm{MPa\,m^{-1}}$) and the matric potential (Ψ_m). As long as Ψ_g is greater than Ψ_m, water will flow downward through the soil. When the gravitational potential is exactly balanced by the soil matric potential, water flow equals zero. The soil's hydraulic conductivity is determined by the pore size distribution and water content. The equation stating this was first derived for saturated materials by Darcy in 1856 (cited by Kelliher and Scotter, 1992) as

$$F = -K_{sat}\,(\Delta\Psi/\Delta z) \tag{2.16}$$

where F is the volume flux of water through unit cross-sectional area per unit time in the direction of the lower potential, and z is the distance. Soil hydraulic conductivity (K) falls rapidly as θ decreases, in the same way as the hydraulic conductivity of sapwood. The unsaturated hydraulic conductivity of soil is very much a function of soil texture and pore

size distribution, which can be described reasonably accurately with empirical equations that are a function of the clay fraction and the ratio θ/θ_{sat} (Clapp and Hornberger, 1978). Alternatively, K can be expressed in reference to changes in Ψ_p (Fig. 2.17). For a pure sand, at saturation, K_{sat}, the maximum sustainable infiltration rate, is above 10,000 mm day^{-1}, whereas for a silt loam with very uniform pore sizes, K_{sat} is only 0.05 mm day^{-1}. A sandy loam with a mixture of large and small pores has an intermediate K_{sat}, around 300 mm day^{-1}. Most undisturbed forest soils have saturated conductivities in their surface horizons above 20 mm hr^{-1} or 500 mm day^{-1}. Approaching the other extreme, minimum flows of less than 1 mm day^{-1} can be expected on all soils once the potential gradient falls below −0.01 MPa (Fig. 2.17).

Saturated and unsaturated hydraulic conductivity are usually estimated from laboratory analyses on undisturbed cores collected at different soil depths (Vepraskas *et al.,* 1991). When soils are variable, many core samples are required. In such cases, field determination of hydraulic conductivity, made on soils as they are wetted and drained, is often more reliable (Luxmoore, 1983; Talsma and Gardner, 1986; Whitehead and Kelliher, 1991).

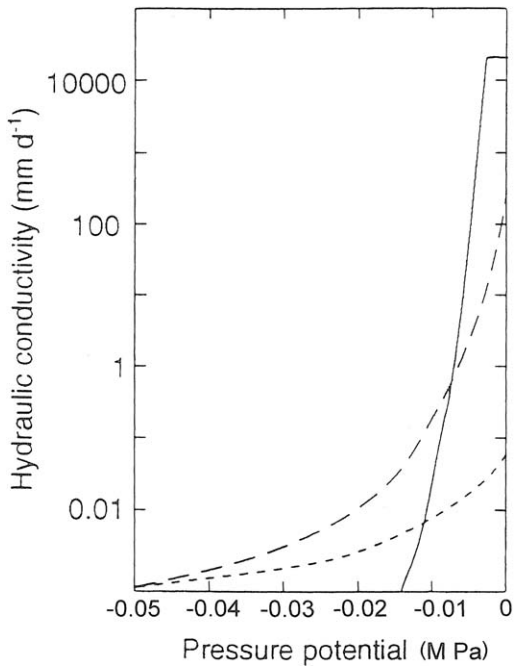

FIGURE 2.17. The hydraulic conductivity of soils decreases rapidly when the volumetric water content drops below saturated, here represented when the pressure potential equals zero. Sandy soils (solid line) exhibit at 0 pressure potential K_{sat} > 10,000 mm day^{-1}. Fine clays or extremely uniform silty soils (- - -) can make a subsoil nearly impervious, with K_{sat} < 0.05 mm day^{-1}. A sandy loam soil (– – –) has a relatively high K_{sat} of 300 mm day^{-1} and the capacity to contribute slowly to subsurface and streamflow as the pressure potential decreases. Below a pressure potential of −0.01 MPa, however, the hydraulic conductivity for most soils falls below 1 mm day^{-1}. (After Kelliher and Scotter, 1992.)

Drainage characteristics change within soil profiles so the flow of water, even in saturated zones, is not uniform. This has led to development of very complicated models, but most are based on some variation of Darcy's law (Golden, 1980; Prevedello *et al.,* 1991).

Deleterious effects of forest practices on surface soil permeability, where most compaction occurs, can be easily measured. Compaction from logging, road building, or heavy grazing can substantially increase the bulk density of surface soils and reduce infiltration rates. As a result of such activities, surface runoff and erosion may be increased by orders of magnitude in steep mountainous areas, particularly those with monsoon climate (Riley, 1984; Gilmour *et al.,* 1987; Kamaruzaman *et al.,* 1987; Malmer and Grip, 1990). If measurements are made of soil hydraulic properties throughout the surface and subsoil, unstable slopes which contain impervious horizons that foster lateral water flow can be recognized before roads and culverts are in place.

In summary, soil texture and soil depth both play an important role in determining the rate at which water flows into streams. Shallow, coarse textured soils store little water and drain rapidly, whereas deep, fine textured soils have the capacity to store large amounts of water and release the excess slowly into groundwater reservoirs and streams. Abrupt transitions in soil texture or bulk density within the profile alter hydraulic properties to cause abrupt changes in lateral flow. As a result, slopes may become unstable and subject to slumping and mass failure when saturated.

VI. COUPLED WATER BALANCE MODELS

We can now assemble the key components of the hydrologic system: precipitation is the input; snow, soil, and sapwood are storage components; and evapotranspiration and runoff are outputs (Fig. 2.18). A variety of forest ecosystem models exist which share a common structure and apply many of the formulas presented in this chapter (Ågren *et al.,* 1991; Whitehead and Kelliher, 1991; Aber and Federer, 1992; McMurtrie, 1993; Williams *et al.,* 1996). These models predict vapor losses in the form of transpiration and evaporation (and sublimation in the case of FOREST-BGC). They all calculate a daily water balance for the soil, but rarely for tree stems (except see Williams *et al.,* 1996). Excess water is routed into seepage or runoff.

Models can be run from daily weather data but are improved when precipitation, solar radiation, temperature, humidity, and wind speed can be provided hourly. In addition to general site descriptors (latitude, elevation, slope, and aspect), knowledge of seasonal changes in LAI is a prerequisite for all integrated ecosystem models. Likewise, some estimates of rooting depth and the water storage and drainage characteristics of soils are essential. Additional structural information is needed if water stored within the sapwood of vegetation is considered, and if the hydrologic responses of separate strata of vegetation are of interest (e.g., height, LAI, leaf dimensions, and rooting depth). The stomatal response of different species to atmospheric humidity deficits and to soil temperature limitations can further improve model results (Körner, 1985; Kelliher *et al.,* 1993; Schulze *et al.,* 1994a).

The most convincing tests of these forest hydrologic models are provided by comparing predicted against observed snowpack dynamics (Fig. 2.16), canopy evapotranspiration (Fig. 2.19a), and seasonal patterns in soil water depletion (Fig. 2.19b). Most models apply

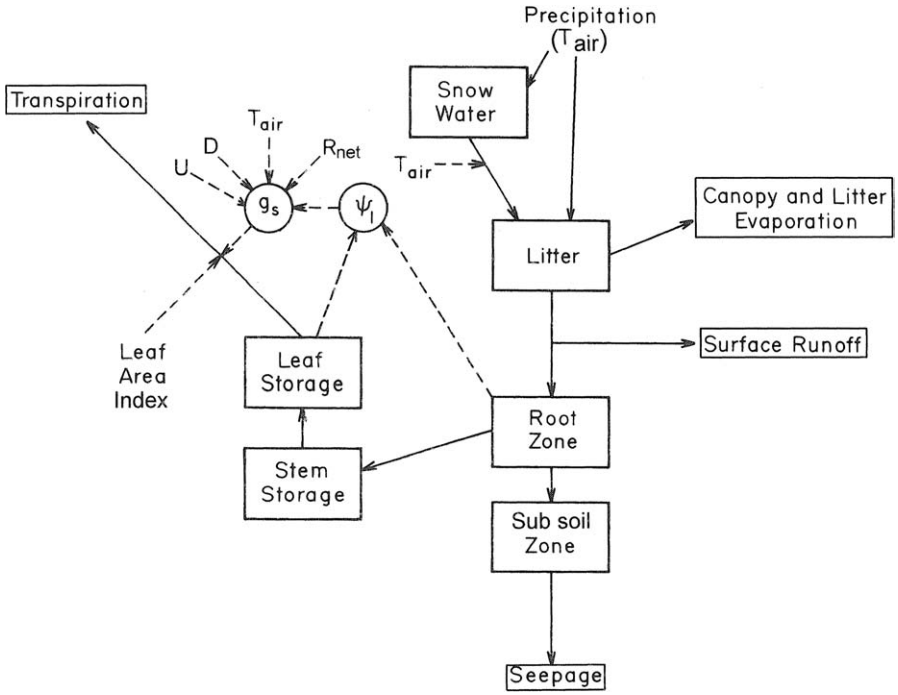

FIGURE 2.18. General structure of a forest water balance model that accounts for precipitation entering a snowpack, litter, soil surface, and subsoil horizons. Water is eventually lost from the system through transpiration, evaporation, runoff, or seepage. Within trees, water may be stored temporarily in the sapwood of stems and branches, and in leaves. Evaporation from wet canopies depends on the driving variables (R_n), wind speed *(U)*. and vapor pressure deficit (*D*) and structural variables associated with height and the leaf area index (LAI) that affect boundary-layer conductance. The calculation of transpiration requires an additional parameter, stomatal conductance (g_s), which reflects all the hydraulic resistances in the path between roots and leaves. Values of leaf water potential (Ψ_l) may be simulated and compared against measurements. A daily estimate of change in each storage compartment represents the finest resolution predicted by most coupled ecosystem models. (Modified from *Oecologia,* "Physiological control of water flux in conifers: A computer simulation model," S. W. Running, R. H. Waring, and R. A. Rydell, Volume 18, p. 11, Fig. 5, 1975, © 1975 by Springer-Verlag; and from Running, 1984a.)

the simple "big-leaf" Penman–Monteith equation and derive estimates of radiation and humidity with climatological models rather than from direct measurement (see Chapter 7 for details). In situations where rooting depth is unknown or difficult to establish, hydrologic models such as FOREST-BGC which predict predawn plant Ψ offer a realistic check on estimates of rooting depth and the amount of water extracted during long periods of drought (Running, 1994).

Modeling the annual water balance with a range of LAI values helps set realistic limits on hydrologic flows. Figure 2.20 shows that where precipitation is high and evenly distributed seasonally (e.g., Jacksonville, Florida, and Knoxville, Tennessee), FOREST-BGC predicts that outflow will drop from 80 to 20 cm as LAI increases from 3 to 9; consequently, streamflow records imply that reasonable maximum LAI values do not exceed 6.

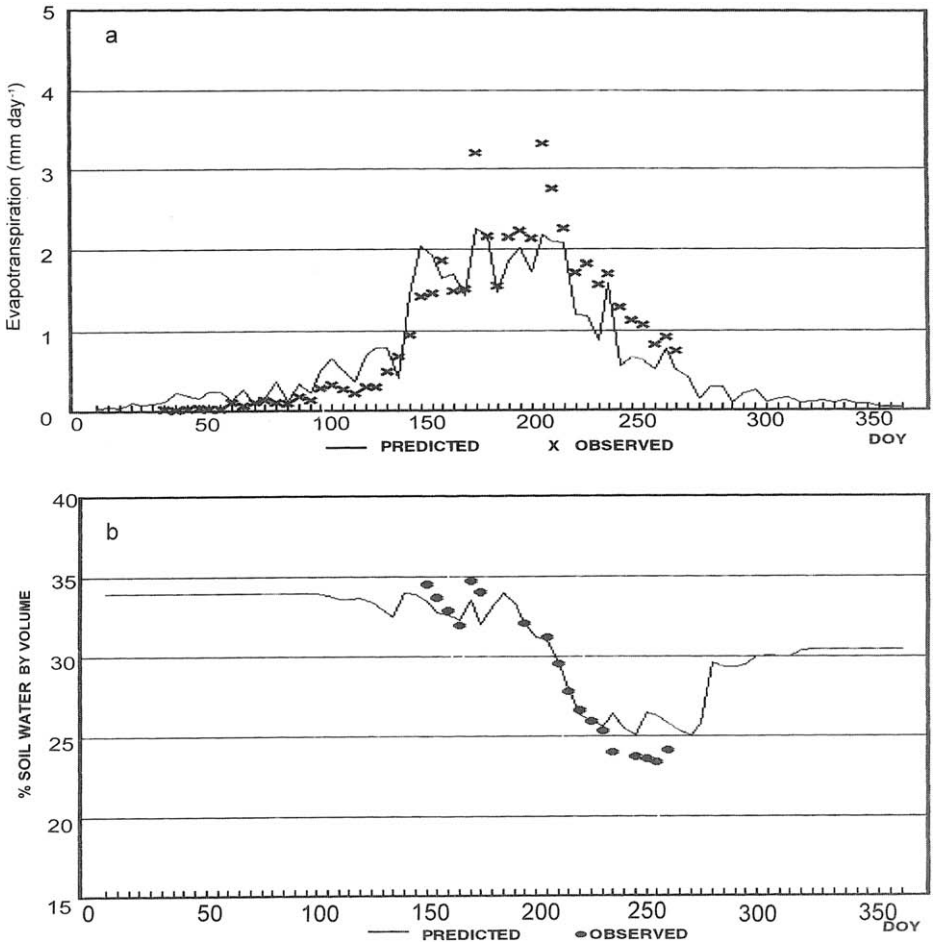

FIGURE 2.19. (a) The FOREST-BGC simulation model (Running and Coughlan, 1988) predicted daily evapotranspiration (continuous line) from an aspen forest that generally agreed with micrometeorological measurements (x) made throughout most days of a year (DOY). (b) Model predictions of soil water depletion also matched those determined with a neutron probe. (After Kimball *et al.,* 1997a.)

In more arid climates (Missoula, Montana; Fairbanks, Alaska; and Tucson, Arizona), no outflow is predicted at the lowest LAI of 3.0; values of 9 are likewise unrealistic in these climates. Direct observations of maximum leaf area index for Missoula, Montana, confirmed that values there were less than 3.0 (Running and Coughlan, 1988). Additionally, in the cold and arid Montana climate, snowpack is more important than soil depth for sustaining forest LAI. At sites with intermediate climates, like Seattle, Washington, and Madison Wisconsin, stream discharge is inversely proportional to LAI, and the distinction between evergreen and deciduous forest cover becomes increasingly important.

Grier and Running (1977) showed that the LAI of mature coniferous forests across the steep environmental gradient associated with the Oregon transect at 44°N (Fig. 1.4) was

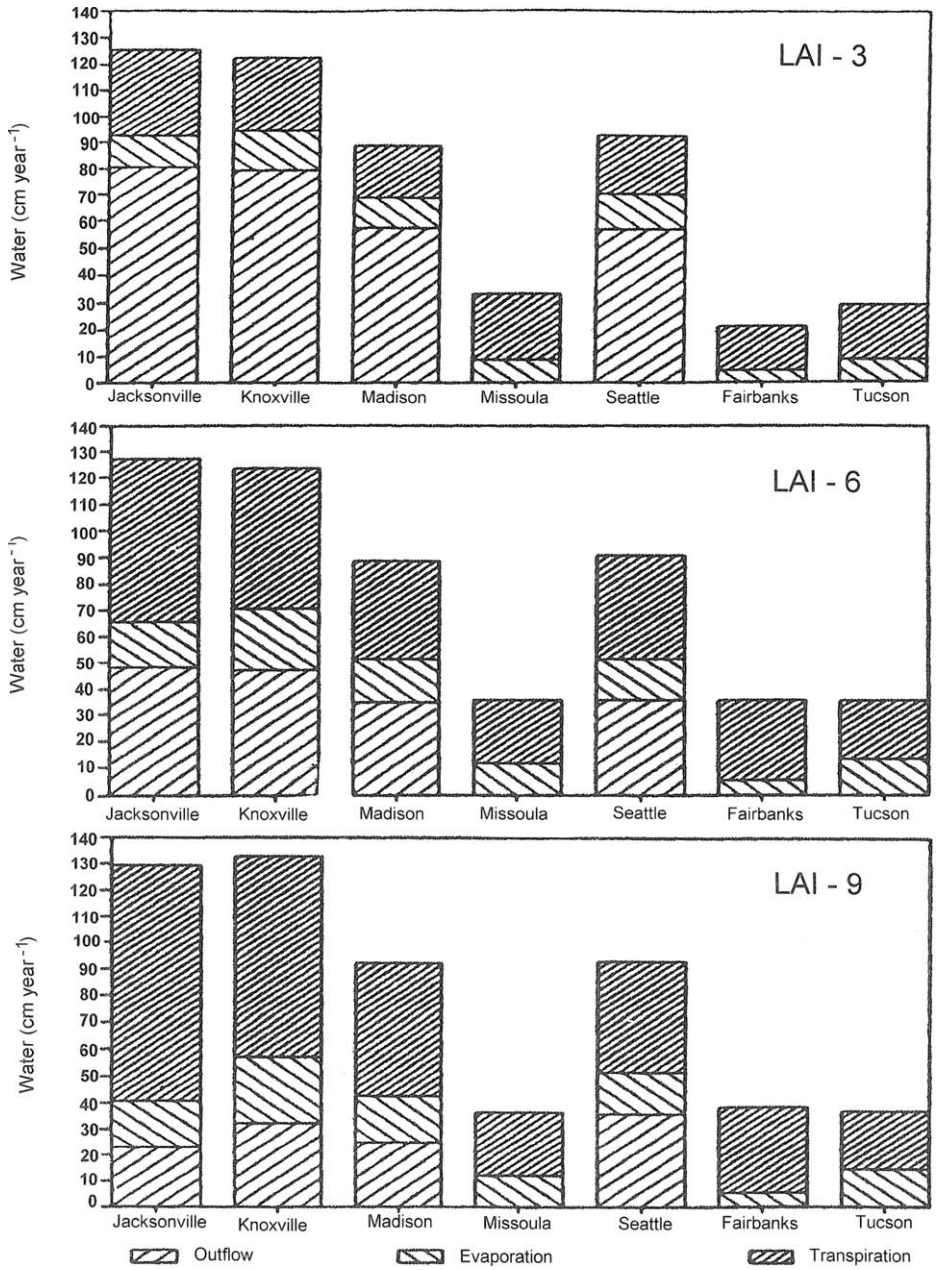

FIGURE 2.20. A sensitivity analysis with FOREST-BGC performed with weather data gathered at different cities throughout the United States indicates that increasing the leaf area index (LAI) from 3 to 9 would affect outflow and other hydrologic losses most on sites which receive >80 cm year^{-1} of precipitation. In more arid environments (Missoula, Montana; Fairbanks, Alaska; and Tucson, Arizona), no outflow is predicted at an LAI of 3. (Reprinted from *Ecological Modelling,* Volume 41, S. W. Running and J. C. Coughlan, "A general model of forest ecosystem processes for regional applications. I. Hydrologic balance, canopy gas exchange and primary production processes," pp. 125–154, 1988, with kind permission of Elsevier Science–NL, Sara Burgerhartstraat 25, 1055 KV Amsterdam, The Netherlands.)

related to site water balance (Fig. 2.21). Specht and Specht (1989) showed a similar sensitivity of eucalyptus-dominated communities in Australia to aridity gradients. Following this type of analysis, Nemani and Running (1989a) built a simplified hydrological equilibrium concept into a model that further quantified the relations among precipitation, soil water storage, and forest LAI. When precipitation and soil water holding capacity are known, they could predict the maximum LAI that a site can support, an important concept in defining potential forest conditions and in evaluating site degradation at larger scales. When the hydrologic components of ecosystem simulation models are linked with carbon balance (Chapter 3), predictions of photosynthesis, respiration, and growth allocations provide additional insights into the limitations on LAI.

Water balance modeling can aid in a number of management decisions, as will be featured in Chapter 8. The hydrologic consequences of forest cutting can be explored before harvesting is initiated to determine potential changes in groundwater recharge and the danger of excessive surface runoff that could increase the probability of downstream flooding. The rate of hydrologic recovery after forest harvesting can be simulated in advance and the influence of vegetation on evapotranspiration and soil compaction separately evaluated. In early estimates of hydraulic recovery based on gauged watersheds (Harr *et al.,* 1979), it was difficult to explain inconsistencies because measurements of LAI, rooting depth, and differences in boundary layer and stomatal conductance were not

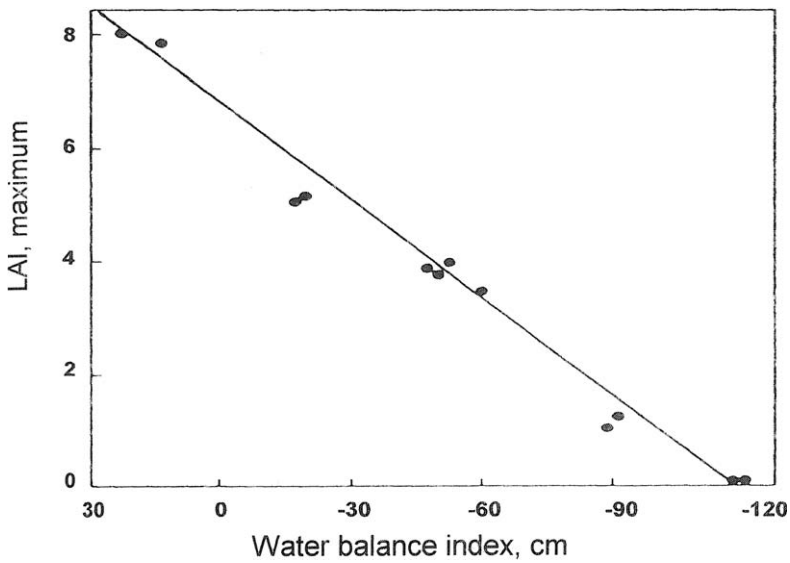

FIGURE 2.21. In the Pacific Northwest, climate and topography vary considerably. As conditions change, so do the species that dominate the forests, as shown in the transect across western Oregon (see Fig. 1.4). The maximum observed leaf area index of the forests ranges from less than 1 to 8 across the transect, correlated with a summer water balance computed by adding soil water storage to measured growing season precipitation and then subtracting open-pan evaporation (data from Grier and Running, 1977; Gholz, 1982). The LAI estimates were converted from all surfaces by dividing by 2.5 and values were resealed by 0.5, based on corrections published by Marshall and Waring (1986) indicating overestimates in the original analyses in 1977.

available. As a result, summer flows could return to normal within a decade while peak flows during storms might remain high for many years, depending on the rate of recovery from soil compaction and reestablishment of conifer LAI. Simulations indicate that 20–30 years should be adequate on most sites in the U.S. Pacific Northwest to permit a return to maximum LAI, and observations substantiate this prediction (Turner and Long, 1975).

VII. SUMMARY

In this chapter we identified the major components of a hydrologic model that can be linked to carbon and nutrient cycling models. Five meteorological variables drive the hydrologic model: solar radiation, temperature, vapor pressure deficits, precipitation, and wind speed. The soil and snowpack are major sources of temporary water storage. The leafy canopy and surface litter present the main surfaces from which water is transpired or evaporated. The vertical height, seasonal variation in LAI, and rooting depth are important properties of vegetation that affect water movement through ecosystems. Seasonal limitations on the source and flow of water from roots through stems and branches can be assessed by monitoring the relative water content of sapwood and its δD, the δ^{13}C of foliage, and the predawn Ψ of twigs. By incorporating additional properties of the soil, hydrologic models have wide application. Such models provide insights into the implications of various policies that alter forest composition and structure.